meteorites tektites impactites

meteorites

EDITOR: Tadeusz A. Przylibski

December 2011

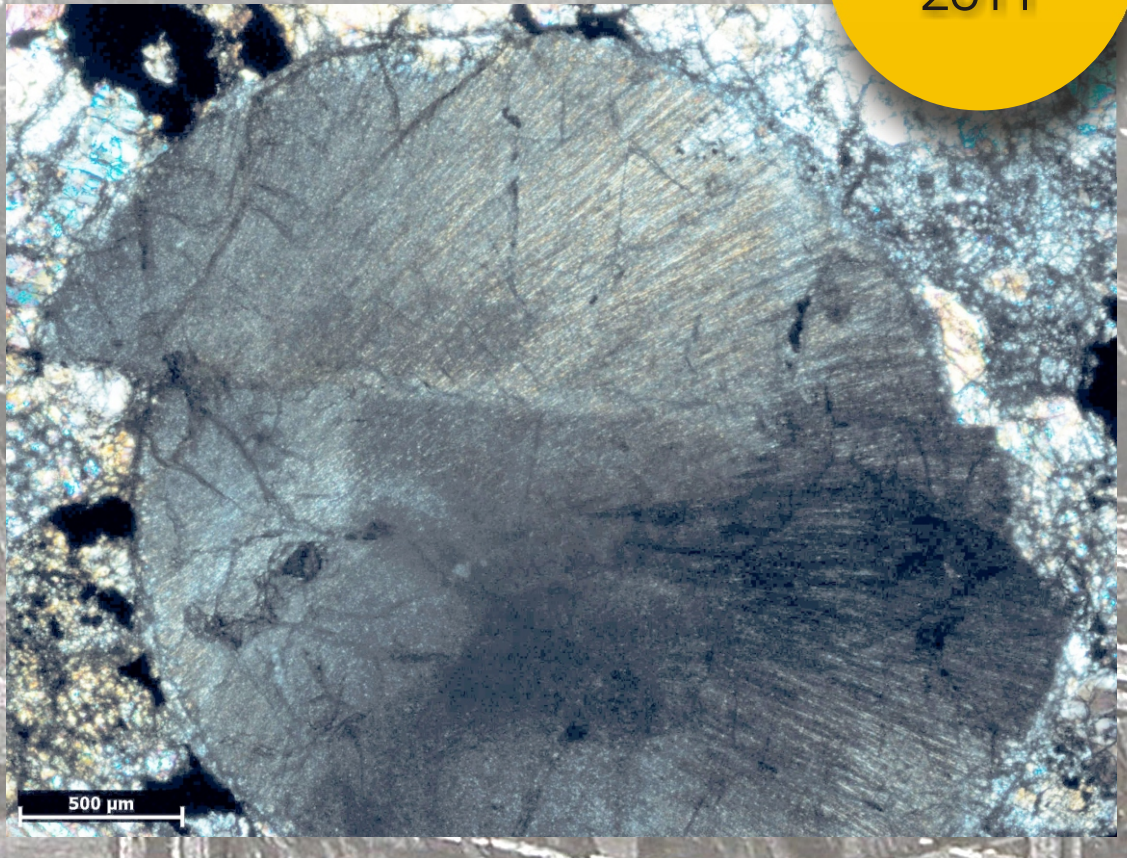

Vol. 1
No. 1

ISSN 2299-0313

www.meteorites.pwr.wroc.pl

meteorites

"The first open-access journal focusing exclusively on meteoritics"

Meteorites Publishers

Wrocław University of Technology
Faculty of Geoengineering, Mining and Geology
Wybrzeże S. Wyspiańskiego 27
50-370 Wrocław, Poland

Polish Meteorite Society
Będzińska 60
41-200 Sosnowiec, Poland

Photo on cover: Shear fracture in a radial pyroxene chondrule from the Pułtusk meteorite. Horsetailing structure at the termination of the fracture occurs. Shear sense is sinistral. Photo Agata Krzesińska

Meteorites
Vol. 1, No. 1, 2011, 1
www.meteorites.pwr.wroc.pl

JOURNAL INFORMATION

Meteorites provides a coherent international forum for the publication of research in the field of meteoritics and its related disciplines. The topics of interest range from, but are not limited to, meteorites and other kinds of extraterrestrial matter and their sources of origin through the examination of the mineral resources of the Solar System, to tektites, impactites, and impact structures.

Meteorites invites the submission of articles covering the broadly defined field of meteorites. In addition to publication of research results, however, authors are encouraged to share and present astronomical, petrological, mineralogical, geochemical, and isotopic data on all groups and types of meteorites. Meteorites is intended to serve as a basic reference source for in-depth analyses and compilations on particular meteorite groups and their parent bodies, as well as the genesis and evolution of the Solar System, as well as other planetary systems.

Considering the progress of human space exploration and conceivable colonization of other planets, this data will likely play an important role in the recognition and exploitation of extraterrestrial mineral resources. Therefore, in light of the potential benefits, Meteorites editors have no intention of rejecting paper submissions pertaining to the research of meteorites with provisional names and pending classifications, esp. prior to their approval by the Committee on Meteorite Nomenclature of the Meteoritical Society.

Meteorites invites the publication of important papers intended as reference sources for other researchers, as well as compilations and interpretations of other works on meteorites of lesser scientific importance and their parent bodies. Not only does Meteorites welcome submissions of research descriptions and results regarding 'rare' meteorites, and topics such as newly-discovered extraterrestrial mineral species, but it also gladly accepts articles covering more common groups of meteorites. Due to their relatively low scientific value in terms of current research trends, many interesting research results are quietly filed away into archives instead of being published in leading scientific journals.

Our intention is not to compete with existing journals, but to add to the currently limited publication space for researches on meteorites. Meteorites editors will gladly accept any reliable research results, including submissions that are virtually impossible to publish in today's existing journals due to the apparent mediocrity of the specimens studied. At Meteorites, we believe that even profoundly studied meteorites can have a significant and relevant bearing on our knowledge and understanding of the solar system. Meteorites will, in time, develop into a repository of data and knowledge available for everyone with an interest in extraterrestrial matter.

Our purpose is to develop a new interdisciplinary journal covering the multitude of subject matters involved in meteorite research. Due to an insufficient amount of publication space, the increasing number of specimens available for research, and a growing list of research centers, only a small percentage of valuable submissions is ever brought to publication.

Through the Open Access publications, Meteorites aims to support academic work and to act as an accessible research data center. Meteorites is available free of charge in print or digital document. Each paper is thoroughly reviewed by experts in the field. Submissions should be sent directly to the e-mail address of the secretary: meteorites@pwr.wroc.pl. Authors are required to follow the guidelines available at http://www.meteorites.pwr.wroc.pl

Meteorites
Vol. 1, No. 1, 2011, 3–12
www.meteorites.pwr.wroc.pl
DOI 10.5277/met110101

HIGH RESOLUTION X-RAY TOMOGRAPHY AS A TOOL FOR ANALYSIS OF INTERNAL TEXTURES IN METEORITES

Agata KRZESIŃSKA[1]

[1] Polish Academy of Sciences, Institute of Geological Sciences, ul. Podwale 75, 50-449 Wrocław, Poland.

Abstract: A comparison of internal textures of the NWA-5929, Ghubara and Pułtusk chondrites has been carried out using high resolution X-ray tomography. This is a powerful, non-destructive technique that allows one to determine textural and compositional differences that occur between ordinary chondrites of various groups by means of grey-level scale histograms, first-order statistics, and 3D imaging.

Deformational structures in the Pułtusk meteorite such as cataclastic zones, impact melt clasts, melt veins, and melt pockets are observed and studied. Measurements of metal particle size are achieved, giving even deeper insight into textural features of meteorite. My approach shows that as shock deformation occurred, numerous small metal grains became progressively dispersed within the volume of the deformed Pułtusk meteorite rock. Simultaneously, metal was mobilized via frictional or direct impact melting to form scarce large metal nodules or grains arranged along the margins of relict chondritic clasts or as components of irregular injection veining.

The possibility of tracing of these impact related processes by using tomography micrograms (without breaking the sample) is very useful for distinguishing which parts of each meteorite were deformed in different ways in order to make first-order observations regarding the deformational history of these meteorites.

Keywords: NWA-5929, Ghubara, Pułtusk, high resolution X-ray computed tomography, deformation

INTRODUCTION

High resolution X-ray tomography (HR XCT) is a non-destructive method of analyzing solid-state bodies. For this reason, it has recently become one of the important tools for studying extraterrestrial materials like meteorites (Rubin et al., 2001; Ebel et al., 2008; Hezel et al., 2010; Kuebler et al., 1999; Nettles & McSween, 2006; Tsuchiyama et al., 2002), Antarctic micrometeorites (Okazawa et al., 2002), interplanetary dust particles, and material from sample-return missions (Nakamura et al., 2008). HR XCT was first utilized by Masuda et al. (1986) to study Antarctic meteorites in which silicates, sulphides and metal particles were distinguished, although no textural information was obtained because attainable resolution was then insufficient (~0.25 mm). The first real textural observations were carried out by Kondo et al. (1997), when they resolved porphyritic chondrules composed of euhedral crystals and surrounded by Fe-rich rims. At that time, however, few works were dedicated to studying the internal textures of meteorites (Rubin et al., 2001; Żbik & Self, 2005) or the potential that HR XCT had for refining the classification of meteorites (Friedrich, 2008).

Textures of meteorites are still usually studied by making thin sections. This necessitates cutting the meteorite to be studied. However, with help of HR XCT, significant data on meteorites' internal texture may be collected without (or before) the partitioning of the sample. This paper shows that, with the aid of HR XCT, it is possible to demonstrate numerous differences between undeformed samples and samples that were cataclased or impact-melted with included metal veins or silicate-melt veins, melt pockets, and metal nodules. Author was also able to make semi-quantitative measurements of the volume of metal particles, allowing for inferences on the deformational processes involved.

Corresponding author: Agata KRZESIŃSKA, agatakrz@twarda.pan.pl

METHOD

The main parameter measured in high resolution X-ray tomography is a linear X-ray attenuation coefficient. In its simplest form, an X-ray fan beam in the tomographic instrument is directed at the object and the decrease in X-ray intensity caused by the passage through the object is measured by a linear array of detectors. The analysed object is rotated as measurements proceed, allowing it to be X-rayed at various orientations. At each rotation angle, the X-ray absorption is recorded and the obtained data are then reconstructed to create a cross-sectional image of the object along any arbitrary plane (Duliu, 1999; Uesugi et al., 2010). The difference of the X-ray absorption appears as the difference of computed tomography (CT) values in the image. A computer-aided generation of the resulting images relies on grey-scale variations within digital representations of the body being studied. The resulting picture is a stack of images of 8-bit 256-grey-scale colours. The grey-scales in such images reflect the relative linear X-ray attenuation coefficient, which is a function of density, atomic number and X-ray energy. When a mineral has larger X-ray absorption (higher X-ray attenuation coefficient) its CT value is larger and its image is brighter. Because the resulting values depend also on X-ray energy, calibration is needed for quantitative analyses.

Based on tomographic reconstructions, grey-level scale statistics were made and volume contents of metal were measured (Friedrich, 2008; Uesugi et al., 2010). In the next step, the HR XCT data were extracted for volumetric representations to obtain information about the shape of some elements and their relationship with their surroundings (Ketcham & Carlson, 2001; Ketcham, 2005; Carlson, 2006). Threshold tomograms were used in these reconstructions. ImageJ® was used as an open source program to manipulate image stacks and ImageJ 3D Viewer plugin was used for volumetric extractions.

Textural maturity descriptors of the analysed samples are based on grey-level co-occurrence matrices (GLCM) of the images (Petrou & Garcia Sevílla, 2006; Friedrich, 2008). The co-occurrence matrix represents the probability of the occurrence of a pair of grey values separated by a distance of 1 voxel at an angle $\Theta = 0°$. Entropy and angular second moment quantify the degree of order within a GLCM. The inverse difference moment and contrast are parameters of the differences of grey-level scale values occurring within a GLCM. GLCM measurements for the analyzed samples are shown in table 1 and they reflect homogeneity of the samples which in turn relate to textural maturity (Petrou & Garcia Sevílla, 2006; Friedrich, 2008).

SAMPLES USED IN EXPERIMENT

Samples of NWA–5929 (75 g) and Ghubara (9.5 g) as well as 23 samples of the Pułtusk meteorite (from 9.5 to 62 g) were analysed using HR XCT. They were analysed in their as-received states in the Institute of Gas and Oil, Kraków. A Benchtop CT160 high-resolution X-ray tomographic system was used in this study. The specimens were rotated 360° with X-ray projection images taken at 1° intervals. The X-ray source was operated at 160 kV. The voxel size (volumetric resolution) in tomography micrograms, determined by the 3D size of each sample, was 28.2 μm, 13 μm and 16.5 – 35.5 μm for the NWA–5929, Ghubara and Pułtusk samples, respectively.

The analyzed samples of Pułtusk meteorite were generously provided by the Museum of the Earth, Polish Academy of Sciences in Warsaw, Mineralogical Museum of the University of Wrocław, The Thugutt Mineralogical Museum on the Faculty of Geology, Warsaw University, Mineralogical Museum of Jagiellonian University in Kraków and the Geological Museum at the Institute of Geological Sciences PAS in Kraków.

NWA-5929 meteorite is an unclassified chondrite composed of well preserved, large chondrules and euhedral grains of olivine and pyroxene. The chondritic matrix is fine grained, composed of silicates and a small fraction of metal-sulfide aggregates. Silicate grains are generally irregularly fractured.

Ghubara, an L-chondrite, was found in 1954 in Oman. It is a brecciated chondrite with several kinds of clasts differing in textures. They range from unequilibrated chondritic material to highly recrystallized, impact-melted and achondrite-like inclusions (Vinogradov and Vdovykin, 1963; Binns, 1967). The analyzed sample contains microcrystalline as well as porphyritic clasts (2–4 mm in size) of impact origin embedded in a highly deformed chondritic L5 host rock (Krzesińska & Siemiątkowski, 2011). The sample is veined and fractured.

The Pułtusk meteorite fell in 1868 in Poland. It is classified as H4-5 chondrite (Binns, 1967; Manecki, 1972) and its shock deformation stage is S3 (Stöffler et al., 1991). It is composed of H4 and H5 clasts. However, the cataclastic texture is overprinted on this

kind of brecciation (Krzesinska, 2010a). Petrography of the samples used in the experiment has already been a subject of analyses. The results suggest that the meteorite experienced a complicated deformational history with impact melting and frictional melting acting during high strain-rate impacts on the parent body of the meteorite (Krzesinska 2010a, b). Impact melt veins and clasts as well as metal veins and nodules are present in samples.

In this paper, the Pułtusk meteorite is studied more intensely than the others because of its much more complicated deformational history. Deformational structures analyzed by using HR XCT are shown with the obtained stack manipulation results. It clearly shows the usefulness of the HR XCT technique for solving some problems of deformational history reconstruction.

Table 1. Grey-level statistics and 3D GLCM texture descriptors calculated for a GLCM created at distance 1 and with the angle 0. Values are in 256 color grey-level scale

	NWA 5929 LL	Ghubara L	Pultusk H
metal volume content	2.3%	4.4%	7.1%
mean grey-level value	112	111	123
standard deviation	10.1	13.8	25
skewness	3.5	0.34	2.34
mode	108	110	107
minimum grey-level value	77	78	79
maximum grey-level value	226	225	255
GLCM			
Angular Second Moment	0.001	0.005	0.004
Contrast	268.553	205.472	354.799
Correlation	0.002	0.002	0.001
Inverse Difference Moment	0.199	0.304	0.137
Entropy	4.222	6.936	7.342

RESULTS

The different minerals present in meteorites appear on tomography micrograms as white, grey and dark colours which correspond to Fe-Ni alloy, troilite and silicates, respectively (Fig. 1). Silicate minerals such as olivine and pyroxene cannot be distinguished because difference in the X-ray absorption rate between them is too small. The same applies to kamacite and taenite.

The classification of meteorites is based on their chemical composition (chemical group) and their textural maturity acquired during the earliest metamorphism of a parent-body (Brearley & Jones, 1998; Van Schmuss & Wood, 1967) as well as later impact deformation (Stöffler et al., 1991). Having taken into account that grey-level scale of tomograms in HR XCT reflects the volume content of the co-existing phases, the first-order statistics of the stacks of images were examined and described. These are the simplest textural descriptors derived from the generation of histogram of the grey-level scales contained within a digital dataset (for details see Petrou & Garcia Sevílla, 2006; Friedrich, 2008; Uesugi et al., 2010). The results obtained for NWA-5929, Ghubara, and Pułtusk are shown below.

On tomography micrograms, more discrete deformational structures were detected. It was possible to distinguish and precisely locate metal nodules, metal-free (achondritic-like) clasts in specimens, as well as melt pockets and silicate melt veins. By taking into account the reduced size and dispersion of Fe-Ni metal grains in some parts of the scanned specimens, it was possible to infer their cataclastic texture.

NWA 5929

Grey-level scale histogram

The sample of NWA 5929 contains a large fraction of chondrules with diameters up to 1 mm. They are particularly visible when encased by metallic rims. The measured metal content is 2.3% by volume. The dimensions of the metal grains (up to 0.5 mm) and their slightly irregular shapes are visible on the tomography micrograms (Fig. 1a). It is also seen that the meteorite contains significant amount of sulphides, though its abundance was not measured volumetrically.

The first-order statistics of the grey-level scale of the stacked images give the simplest textural descriptors. They are derived from the histogram of grey-level scale (Fig. 1d). Values are presented in table 1. The mode value – the grey-level value that occurs most frequently (108) is related to silicates, the dominant phase of the sample. The mean value (112) is only slightly higher than the mode, which indicates that the fraction of other minerals in the sample is not significant. The standard deviation (10.1) shows, however, that there are many particles with significantly higher grey-level value than the mean. All of these parameters corroborate what was already known, that the meteorite is generally composed of silicates with small fractions of sulphides and metal.

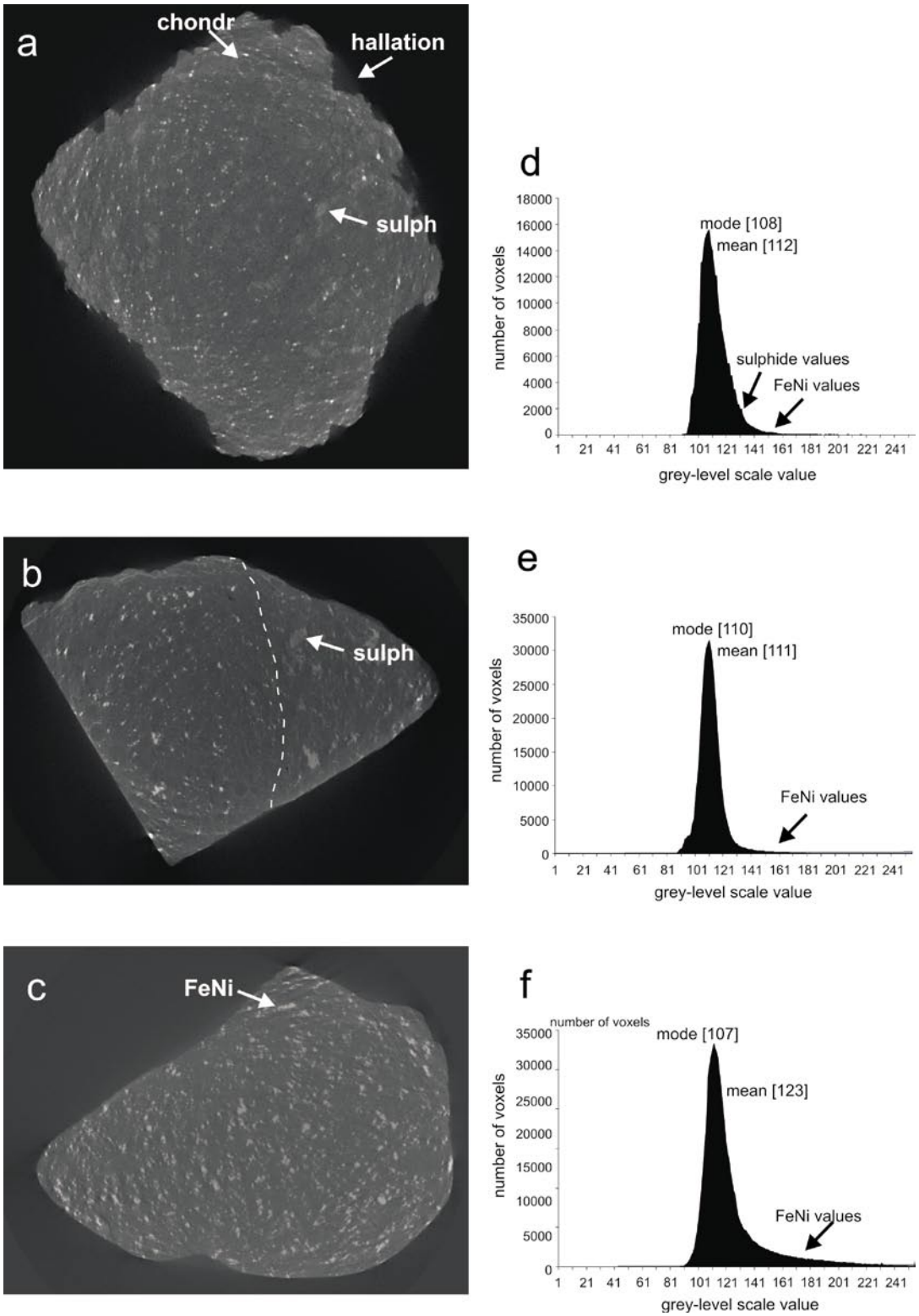

Fig. 1. Examples of tomography micrograms of the NWA-5929 (a), Ghubara (b) and Pułtusk (c) meteorites. Tomography micrograms are constructed in 256- grey-level scale colours. Higher average atomic weight materials (metal) are brighter in the image. Background of an image is the darkest area as the air which surrounds chondrite is characterized by the least X-ray attenuation. Silicates are dark grey, sulphides are medium grey. Histograms of grey-level scale values for NWA-5929 (d), Ghubara (e), Pułtusk (f) meteorites. The mode and mean values are pointed by arrows. Metal-values region is also shown and it is more represented in Pułtusk than in NWA-5929 and Ghubara.
chondr – chondrule; sulph – sulphide; FeNi – metal; hallation – an artifact due to irregular shape of the sample.

GLCM parameters show a low degree of order in the sample (angular second moment = 0.001 and entropy = 4.222; Tab. 1) that suggests low textural maturity and metamorphic equilibration of the sample.

Ghubara

Grey-level scale histogram

The sample of Ghubara contains two different lithology types (Fig. 1b): one with abundant metal particles, and the other with many sulphides grains. Metal content by volume for the whole sample is 4.4%. The statistics of the grey-level scale is shown in table 1. The values are comparable with those obtained for NWA 5929, though the sulphide fraction is less represented on the histogram (Fig 1e), indicated by the higher value of the standard deviation (13.8).

GLCM measurements show a high degree of order as the values of angular second moment and entropy are high (0.005, 6.936, respectively; Tab. 1). These suggest that the sample exhibits a higher degree of textural maturity. It is probably an equilibrated, high petrologic type.

Pułtusk

Grey-level scale histogram

Tomography micrograms of the Pułtusk meteorite show a large amount of metallic particles (Fig. 1c) and small fraction of sulphides. Sulphides generally form rare larger grains or nodules. The measured metal volume content amounts to 7.1%.

A large volume of metal is also seen in the grey-level scale histogram (Fig. 1f) and in the first-order statistics. The mean value of 123 is significantly higher than the mode value, ~107. This parameter and the high standard deviation (25) suggest large fraction of metallic particles.

GLCM descriptors show the homogeneous nature of the studied samples and point to their equilibration (Tab. 1). It was not possible to distinguish between H4 and H5 type material although clasts of the two types are present in the Pułtusk meteorite (Binns, 1967; Manecki, 1972).

Metal nodules and veins

In the analyzed samples, metal nodules and veins occur abundantly yet the volumetric metal content does not differ significantly between samples (Tab. 2). A visualization of the metallic bodies allowed for the determination of their shapes and spatial arrangements and further permitted inferences on their relationships with adjacent silicates. Examples of extracted metal nodules and veins are shown in figure 2.

Generally, nodules that occur in Pułtusk have irregular shapes and display two different textures: massive (Fig. 2a and 2b) and spongy (Fig. 2c). Although cross-sections through the massive nodules are elliptical, they are actually not ellipsoidal in 3D. An example of their interface with silicates is shown in figure 2b. Massive nodules are flattened and pinned by silicates, but the silicates are never embedded in the metal. In contrast, spongy nodules are characterized by the presence of many anhedral silicate grains dispersed in metal (Fig. 2c). The spongy nodule closely examined forms many injections into the surrounding silicate matrix, effectively blurring the boundary between silicates and metal. In figure 2c, the nodule is located close to the fusion crust, however it penetrates deeply into the meteorite, with no relation to surface melting due to the stone's passage through the atmosphere.

Metal veins are also common in Pułtusk. They usually form planar sheets that continue sometimes as silicate-melt veins. Sets of parallel veins are visible in some specimens (Fig. 2d). Visualization of the metallic veins (Fig. 2e) allows obtaining information about their shape. The vein shown on figure 2d is displaced and bent due to dragging along the fault surface. Remobilization of metal into fractures must have occurred as prompted by the irregular shape of the vein. Such observations suggest that deformational processes operated in two stages: 1) emplacement of metallic veins and 2) displacements of plastically behaving veins and remobilization of melt forcibly injected into fractures.

Cataclastic zones

In general, cataclasis in chondrites is connected with the process known as darkening (Rubin, 1992; van der Bogert et al., 2003) which includes melting and dispersion of metal particles in the silicate matrix. Cataclastic portions of studied meteorites can be identified via the presence of small metal grains dispersed throughout the silicate matrix. Many samples of Pułtusk display darkening suggestive of cataclastic zones. In the cataclased domains, dimensions of metal particles were measured and they are shown in figure 3e and in table 2. Comparisons with the same measurements from undeformed samples demonstrate the presence of predominantly smaller grains near voxel size with a few larger metal nodules inside cataclastic domains.

Impact melt clasts and veins

Impact melt rock occurs only in one of the analysed samples, but many impact melt veins and melt pockets were detected in others samples. Because impact melt is composed of dispersed metal particles, the ma-

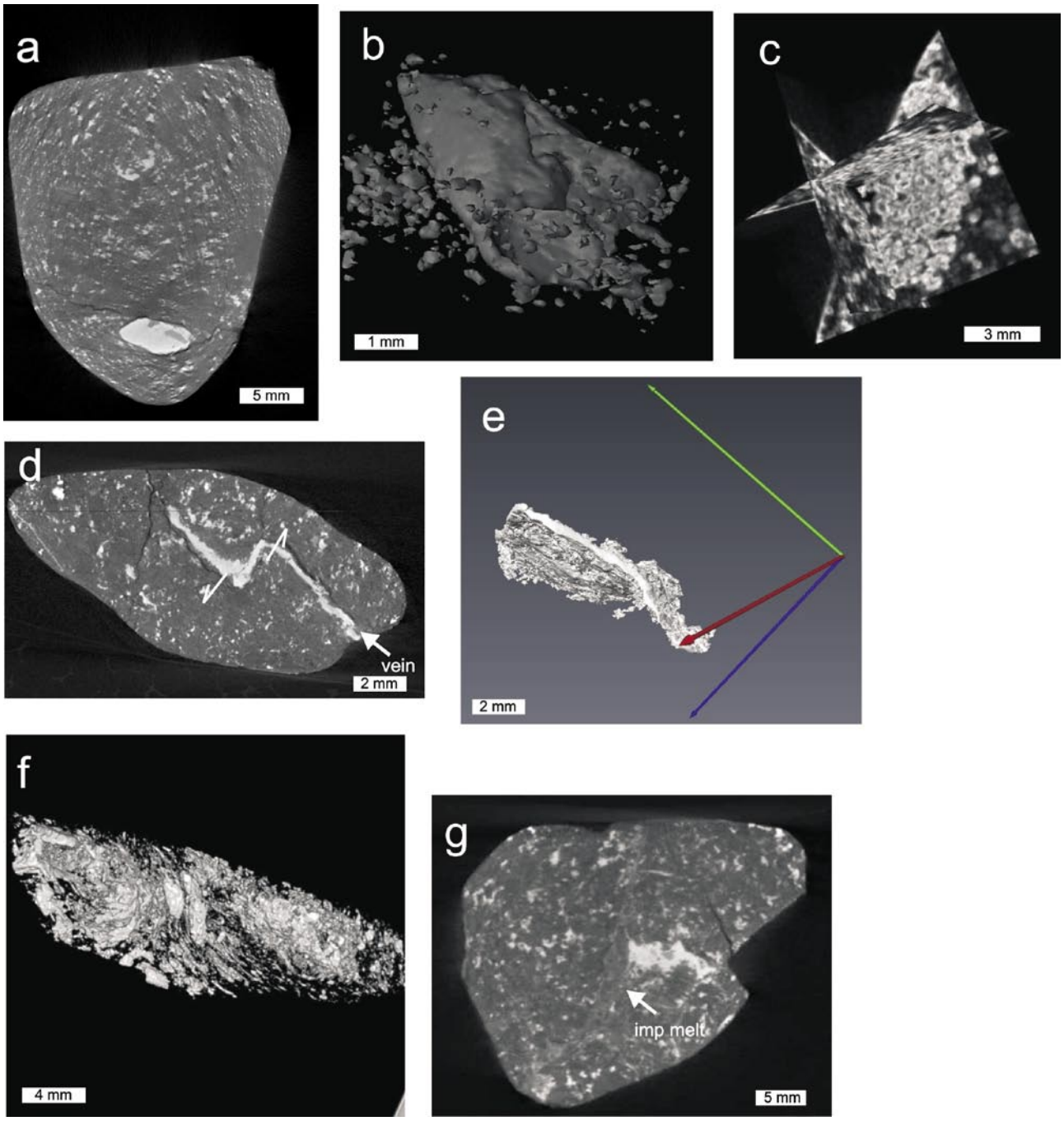

Fig. 2. Visualisation of deformational structures. The deformed bodies are extracted from the volumetric representation of Pułtusk samples; a – tomogram of the massive metal nodule; b – extracted nodule showing the contact with the matrix; c – spongy metal nodule with the silicates embedded into metal alloy; d – tomogram containing the metallic vein; e – extracted vein material showing its contact with the silicates and its geometry; f – extracted metal grains of impact-melt rock, flow-textured arrangement around chondritic relict clasts is pointed out; g – anastomosing impact melt veins in chondritic lithology and remobilized metal grains along the vein. Contrast is enhanced

jority of which are well below voxel size, the resulting grey-scale value is the mean for silicates and metals. Impact melt forms areas of light-grey colour on the tomography micrograms. By enhancing the contrast of the image, the presence of melt can be seen very distinctly. Figure 2g shows an example of an impact melt vein with anastomosed and embeded silicate clasts. Deformational evidence of the remobilization of metal grains along veins is also visible.

The most obvious textural evidence for impact melting is the flow-allignment of melted particles. This can be detected by sight, as shown in figure 2f. Large, elongated metal particles are arranged around clasts of unmelted and not deformed, chondritic material. Taking into account the mean grey-scale value of the phase between clasts, author inferred that the impact melt with metal surrounds chondritic clasts.

Progress of deformational processes – particle size histograms

In this study, volumetric analyses of all metal particles were performed in the not deformed, cataclased, and impact-melted samples of the Pułtusk meteorite. The results are shown in cumulative histograms in figures 3d-f and in table 2.

Dimensions of metal particles changed significantly as deformation and melting progressed. In the cataclased and impact-melted domains, the minimum size of the measured metal particles decreases to 1 voxel size $(20\ \mu m)^3$ and for not deformed samples the smallest metal particles are ~8 times the voxel size in diameter. Particles smaller than 1 voxel in diameter may be escaping our observation in the impact-melted regions because they are near the resolution limit for this technology. However, the volume of particles omitted from the analysis can not be large, because the whole sample volume metal content seems to not be affected.

In spite of the large fraction of small particles in cataclased and impact melted samples, some large metal grains appear. These metal grains are one order of magnitude larger than the largest ones in the undeformed sample. In the cataclased domains, the maximum measured value represents the size of a single anomalously large metal nodule. Within the impact melt, there are flow-arranged, elongated grains. The number of large metal particles is, however, small. As can be seen in figures 3e and 3f, grains with a volume higher than 100 voxels make no more than 1% of the measured particles in the samples.

Table 2. Measured metal particle size distribution in samples of Pułtusk meteorite. Values are in voxel size, what is $(20\ \mu m)^3$

	undeformed sample	cataclased sample	impact melt rock
minimum	8	1	1
maximum	126 482	2 473 500	2 676 656
median	85	64	22
mean value	916	714	467
metal volume content %	7.2%	7.1%	7.7%

Although the biggest metal grains are much larger in the deformed samples than in the undeformed ones, the median value of metal particle size decreases with increasing deformation, whereas the half of the measured particles is smaller than the median. This has to be related to the large fraction of small metal particles in deformed samples. Because the median value decreases with increasing deformation, the number of small dispersed metal grains also increase with the degree of deformation. As the total volume of metal does not change in the analyzed samples, these testify melting and remobilization of metal alloy during deformational processes to voluminous, scarce metal grains and more and more dispersed small metal particles.

DISCUSSION

The presented results of high resolution X-ray tomography measurements show that the volume of metal particles differs distinctly between the Pułtusk, NWA–5929, and Ghubara chondrites (Tab. 1). Moreover, the sulphide phase is more abundant in NWA–5929 than in Pułtusk. This may reflect decrease in overall metal volume and an increase of sulphide phases from the H- to L-chondrites (Brearley and Jones, 1998). The measured metal content value for the NWA-5929 chondrite proves it is an LL/L chondrite.

The measured metal content for the Pułtusk meteorite samples used is 7.1–7.7 vol%. The metal content of Pułtusk was previously measured via HR XCT (Żbik and Self, 2005) and the achieved value 7.7 vol. % correlates well with the results of this study.

The data shown in histograms (Figs. 1d–f) and in the digital set reflect the differences in the content of silicates, sulphides and metal phases, yet point to overall similarities in mineral composition with silicates as the dominant phase. With the same minimum, maximum and mode values of intensity in grey-level scale (the all studied samples are composed of the same minerals, mainly of silicates), the mean value apparently increases from the relative lowest in NWA–5929 and Ghubara to the highest in the Pułtusk chondrites (Tab. 1). It is shown that grey-level scale histograms and statistics estimated from image stacks reflect changes in the mineralogy of meteorites. However, it is important to keep in mind that the value of the grey scale depends not only on the phase composition but also on the X-ray energy. So, only semi-quantitative results are obtainable.

HR XCT technique can provide useful and significant information about the internal textures of meteorites. It provide us with a new and nondestructive means of assigning chondrites to their proper chemical groups as well as providing us with additional information on their metamorphic histories and textural maturity. However, comparison of the petrographic and microstructural analyses of Pułtusk (Krzesinska, 2010a, b) and Ghubara (Krzesińska & Siemiątkowski, 2011) meteorites clearly shows that one cannot reliably distinguish between petrologic types with this technique.

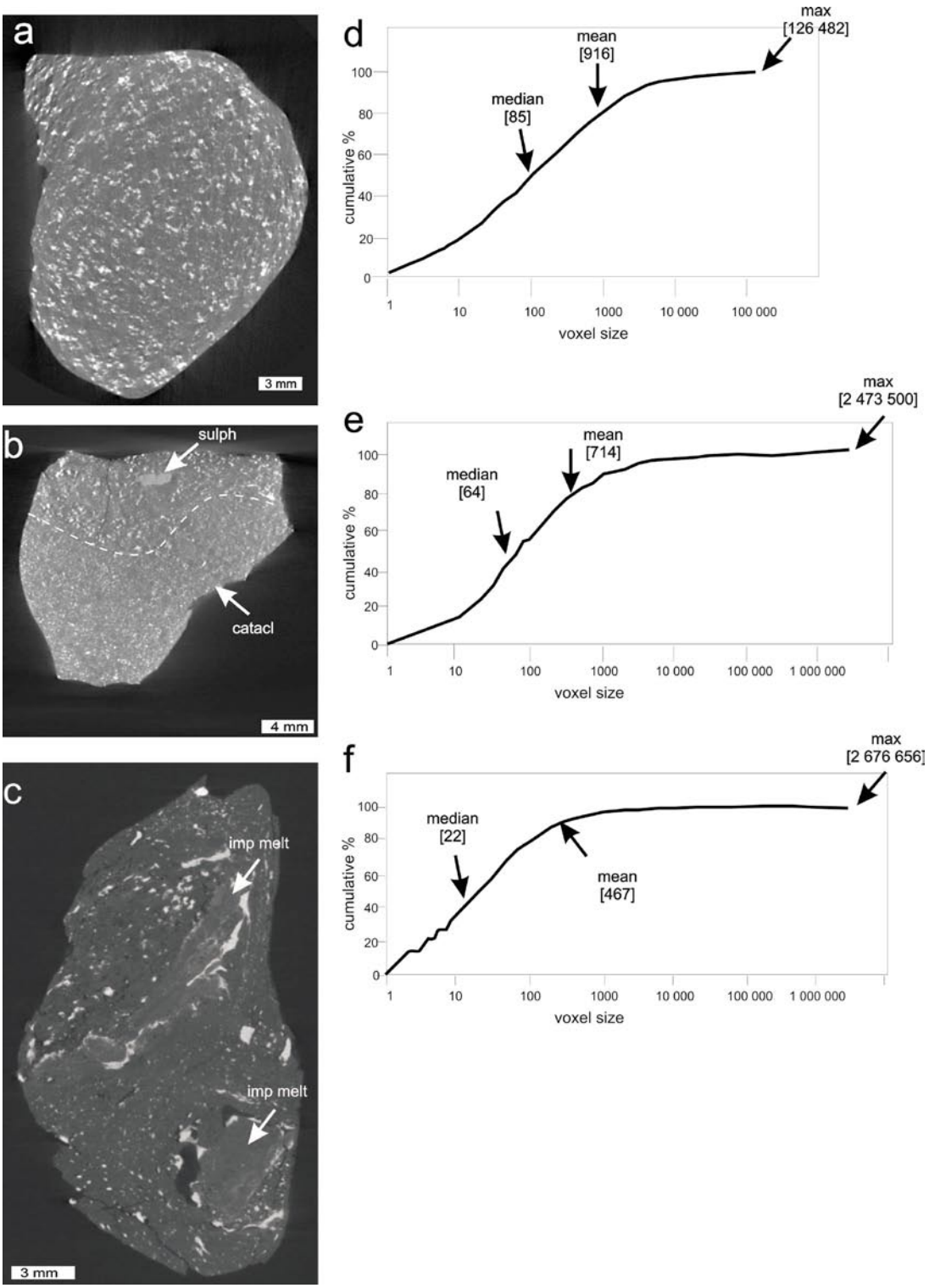

Fig. 3. Tomography micrograms of specimens of the Pułtusk meteorite. a – not deformed, b – cataclased, c – impact melted. Cumulative histograms of metal particle size in these samples: d – not deformed, e – cataclased, f – impact-melted. The size of particles is in voxel size (20 μm)^3. The mean size decreases with the progress of deformation and melting and concurrent formation of large but scarce metallic particles. These large grains are metal nodules and flow-textured remobilized metal grains within the melted domains. Statistical values are shown on histograms and in table 2

Comparison of textural analyses of Pułtusk samples (Krzesinska, 2010b) with HR XCT results shows that using this technique it is possible to trace deformational processes like cataclasis, impact-melting, veining, and metallic melt remobilization. Moreover, HR XCT technique enable us to identify the strong negative correlation between the degree of shock-induced deformation of chondritic meteorites with the size of the metal particles they contain.

CONCLUSIONS

In principle, HR XCT can be used to examine structures of any chondrite component which possesses an X-ray attenuation different from its surrounding material. It is a semi-quantitative tool useful for the chemical classification of chondrites.

By using HR XCT we can trace several processes such as cataclasis (Figs. 3b, 3e), impact melting (Figs. 2f, 3c, and 3f), fracturing (Fig. 2d), formation of melt pockets (Fig. 2g), and metal veins (Figs. 2d, 2e) and nodules (Figs. 2a–c). HR XCT also allows for the semi-quantitative characterization of the size and shape of metal particles (Figs. 3d–f) and voids, and further permits us to make suppositions about the spatial arrangement of deformed areas and, in some cases, to draw conclusions about the sequence of deformational events.

This study is important because it shows that such information can be obtained without sample destruction, in their as-received state. The obtained images may furnish information about textural and compositional features of objects as small as few micrometers, depending on resolution. However, the technique is not without limitation, as the computed tomography can only be used for the study of small samples (up to ~70 g) of meteorites. Despite this limitation, HR XCT technique proves to be a powerful tool, particularly indispensable for studying the textural characteristics of meteorites, and it holds obvious advantages as a non-destructive method.

ACKNOWLEDGMENTS

This research was funded by the Ministry of Science and Higher Education of Poland as a part of the project N N307 474838. The analysed samples of the Pułtusk meteorite were generously provided by the Museum of the Earth, Polish Academy of Sciences in Warsaw, Mineralogical Museum of the University of Wrocław, The Thugutt Mineralogical Museum of the Faculty of Geology, Warsaw University, Mineralogical Museum of Jagiellonian University in Kraków and the Geological Museum at the Institute of Geological Sciences PAS in Kraków. I would like to thank Dr. Tomasz Jakubowski for donating the sample of NWA 5929 chondrite for analysis. Mgr Marek Dohnalik and mgr Jan Kaczmarczyk are thanked for tomographic scanning of the samples. Prof. Andrzej Żelaźniewicz is acknowledged for improvement of the early version of the manuscript. Prof. Ryszard Kryza and Anonymous Reviewer are thanked for careful and helpful review and suggestions that improved the manuscript.

REFERENCES

Binns R.A., 1967 – Cognate xenoliths in chondritic meteorites: examples in Mezo-Madras and Ghubara. *Geochimica et Cosmochimica Acta*, 32 (3), 299–317.

Brearley A.J., Jones R.H., 1998 – Chondritic meteorites. [in:] Planetary Materials, Rev. in Min., 36 (ed. J.J. Papike), 3-1–3-398.

Carlson W.D., 2006 – Three-dimensional imaging of earth and planetary materials. *Earth and Planetary Science Letters*, 249 (3-4), 133–147.

Duliu O.G., 1999 – Computer axial tomography in geosciences: an overview. *Earth-Science Reviews*, 48 (4), 265–281.

Ebel D.S., Weisberg M.K., Hertz J., Campbell A.J., 2008 – Shape, metal abundance, chemistry, and origin of chondrules in Renazzo (CR) chondrite. *Meteoritics & Planetary Science*, 43 (10), 1725–1740.

Friedrich J.M., 2008 – Quantitative methods for three-dimensional comparison and petrographic description of chondrites. *Computers & Geosciences* 34 (12), 1926–1935.

Hezel D.C., Needham A.W., Armytage R., Georg B., Abel R., Kurahashi E., Coles B.J., Rehkaemper M., Russell S.S., 2010 – A nebula setting as the origin for bulk chondrule Fe isotope variations in CV chondrites. *Earth and Planetary Science Letters,* 275 (1–2), 132–180.

Ketcham R.A., 2005 – Three-dimensional grain fabric measurement using high-resolution X-ray computed tomography. *Journal of Structural Geology,* 27 (7), 1217–1228.

Ketcham R.A., Carlson W.D., 2001 – Acquisition, optimization and interpretation of X-ray computed tomographic imagery: applications to the geosciences. *Computers & Geosciences,* 27 (4), 381–400.

Kondo M., Tsuchiyama A., Hirai H., Koishikawa A., 1997 – High resolution X-ray computed tmographic (CT) images of chondrites and chondrules. *Antarctic Meteorite Research*, 10, 437–447.

Krzesińska A., 2010a – Polyphase deformation of the Pułtusk meteorite. Meteoryt, 75 (3), 3–6 (in Polish).

Krzesinska A., 2010b – Oblique impact-induced (shock-related) shearing and frictional melting in Pultusk (H5) chondrite. 41st Lunar and Planetary Science Conference. Abstract #1140. CD-ROM.

Krzesińska A., Siemiątkowski J., 2011 – Evidence for multiple deformational brecciation and impact melting in chondrites from the Jacek Siemiątkowski collection. *Przegląd Geologiczny*, 59 (8), 576–588 (in Polish with English summary).

Kuebler K.E., McSween H.Y., Carlson W.D., Hirsch D., 1999 – Sizes and masses of chondrules and metal-troilite grains in

ordinary chondrites: possible implications for nebular sorting. *Icarus*, 141 (1), 96–106.

Manecki A., 1972 – Mineralogical-petrographic study of the Pułtusk meteorite. *Prace Mineralogiczne PAN*, 27, 53–69 (in Polish).

Masuda A., Taguchi I., Tanaka K., 1986 – Non-destructive analysis of meteorites by using a high-energy X-ray scanner. Papers presented to the 11th Symposium on Antarctic Meteorites. March 25–27, 1986. Tokyo, Nat. Inst. Polar. Res., 148-149.

Nakamura T., Noguchi T., Tsuchiyama A., Ushikubo T., Kita N., Valley J.W., Zolensky M.E., Kakazu Y., Sakamoto K., Mashio E., Uesugi K., Nakano T., 2008 – Chondrule like objects in short period comet 81P/Wild 2. *Science*, 321 (5896), 1664–1667.

Nettles J.W., Mc Sween Jr. H.Y., 2006 – A comparison of metal-troilite grain size distribution for type 3 and type 4 ordinary chondrites using X-ray CT data. *Lunar and Planetary Sciences Conference* XXXVII, abstract #1996.

Okazawa T., Tsuchiyama A., Yano H., Noguchi T., Osawa T., Nakano T., Uesugi K., 2002 – Measurement of densities of Antarctic micrometeorites using X-ray microtomography. *Antarctic Meteorites*, 9, 79–96.

Petrou M., García Sevilla P., 2006 – Image Processing: dealing with Texture. Wiley, New York. 618.

Rubin A.E., 1992 – A shock-metamorphic model for silicate darkening and compositionally variable plagioclase in CK and ordinary chondrites. *Geochimica et Cosmochimica Acta*, 56 (4), 1705–1714.

Rubin A.E., Ulff-Møller F., Wasson J., Carlson W.D., 2001 – The Portales Valley meteorite breccia: Evidence for impact-induced melting and metamorphism of an ordinary chondrite. *Geochimica et Cosmochimica Acta*, 65 (2), 323–342.

Tsuchiyama A., Nakamura T., Nakano T., Nakamura N., 2002 – Three-dimensional description of Kobe meteorite by micro X-ray CT method: possibility of three-dimensional curation of meteorite samples. *Geochemical Journal*, 36 (4), 369–390.

Stöffler D., Keil K., Scott E.R.D., 1991 – Shock metamorphism of ordinary chondrites. *Geochimica et Cosmochimica Acta*, 55 (12), 3845–3867.

Uesugi M., Uesugi K., Oka M., 2010 – Non-destructive observation of meteorite chips using quantitative analysis of optimized X-ray micro-computed tomography. *Earth and Planetary Science Letters*, 299 (3-4), 359–367.

van der Bogert C.H., Schultz P.H., Spray J.G., 2003 – Impact-induced melting in ordinary chondrites: a mechanism for deformation, darkening, and vein formation. *Meteoritics & Planetary Science*, 38 (10), 1521–1531.

Van Schmuss W.R., Wood J.A., 1967 – A chemical–petrologic classification for the chondritic meteorites. *Geochimica et Cosmochimica Acta*, 31 (5), 747–765.

Vinogradov A.P., Vdovykin G.P, 1963 – Diamonds in stony meteorites. *Geochemistry*, 8, 743-750.

Żbik M., Self P., 2005 – High resolution X-ray microtomography analysis in non-destructive investigation of internal structure in two chondrites. *Mineralogia Polonica*, 36 (1), 5–19.

Publishers: Wrocław University of Technology, Faculty of Geoengineering, Mining and Geology
Polish Meteorite Society

Meteorites
Vol. 1, No. 1, 2011, 13–19
www.meteorites.pwr.wroc.pl
DOI 10.5277/met110102

NANOMETER-SIZED MINERAL GRAINS AND THEIR GENETIC TYPES IN METEORITES

Vira P. SEMENENKO[1], Aelita L. GIRICH[1], Kyrylo O. SHKURENKO[1], Natalia V. KYCHAN[1], Svitlana N. SHYRINBEKOVA[1], Tetiana M. GOROVENKO[1]

[1] Institute of Environmental Geochemistry, National Academy of Sciences of Ukraine, Palladina 34a, Kyiv-142, 03180, Ukraine

Abstract: Three genetically different types of nanometer-sized mineral grains in meteorites can be distinguished based on literature and original data: (a) primitive condensates, (b) metamorphic grains, and (c) weathering products. The first of these groups were formed by condensation in a gas-dust nebula in either a presolar or solar environment. Metamorphic grains were formed as a result of thermal, shock or aqueous metamorphism on the meteorite parent bodies. The third type can clearly be characterized as terrestrial weathering products, which are generally found in meteorite finds and are rare or absent within meteorites recovered shortly after having fallen. Nanometric components are found predominantly within the fine-grained silicate material of primitive meteorites. It is suggested that enhanced accretional properties of nanometer-sized grains could be responsible for the primary accretion of condensed nanoglobules within a protoplanetary nebula.

The nature of nanometer-sized inclusions of native W and native Ag originally discovered in the Krymka chondrite is preliminarely discussed.

Key words: meteorite, mineral, genetic type, nanometer-sized grain, origin.

The search for and study of the precursors of primary mineral dust formed within the protoplanetary nebula is important if we hope to decipher the nature of the building materials of the solar system planetesimals and planets. Unequilibrated carbonaceous, ordinary, enstatite and Rumuruti chondrites (e.g., Brearley & Jones, 1998; Bischoff et al., 2011) are important rocks that contain fine-grained materials consisting of both primitive and processed dust (Zinner, 2004; Brearley, 1996). The evolutionary path of this material is extremely complex, since it is relatively unequilibrated and formed under a wide range of PT-conditions. These PT-conditions may have fully or partially changed the chemical and/or mineralogical characteristics of the primary components within the protoplanetary nebula and subsequently within the parent bodies of meteorites.

A comparison of the major mineralogical characteristics of meteorites and terrestrial rocks indicates grain size as one of the distinguishing features resulting from the nature of minerals formed under different PT-conditions. Most terrestrial rocks have variable grain sizes ranging from fine to coarse-grained, although individual crystals can be very large, i.e. more than 1 m. For example, the largest quartz crystal found in Namibia, is ~50 m in size (Bukanov, 2001). In meteorites, the range of grain sizes is much narrower than in terrestrial rocks, and tends to be at the small end of the size distribution for individual crystals. In many extraterrestrial rocks mineral grains larger than 0.5 mm are rare. Complex processes of mineral formation (e.g., condensation, crystallization) and long-term evolution (e.g., thermal and shock metamorphism, aqueous alteration) in the gas-dust nebula, within

Corresponding author: Vira P. SEMENENKO, virasem@i.ua

meteorite parent bodies, and on Earth resulted in the formation of different genetic types of nanometer-sized grains representing an initial stage of structural ordering of solid matter. Using literature and original data, we define three major, genetically different types of nanometer-sized mineral grains in meteorites (e.g., Semenenko et al., 2010): (a) primitive condensates, (b) metamorphic, and (c) weathering.

A. PRIMITIVE CONDENSATES

Currently known isotopic data prove the existence of two major groups of mineral condensates: one group of presolar origin, and the other of solar origin (e.g., Lodders & Amari, 2005; Nittler et al., 2008; Zinner, 2004). The former assemblage is represented by a very small abundance of tiny minerals (Fig. 1a) in primitive chondrites including diamond, silicon carbide, silicon nitrides, Ti-, Zr-, Mo-rich carbides, oxides of Al and Ti, and silicates. Grain sizes of the presolar condensates vary from approximately nanometers to tens of micrometers. The largest presolar minerals are SiC-grains and graphites, which have been found existing with diameters in the μm-range. Other presolar grains are considerably smaller and are not larger than a few hundred nanometers. The smallest of these grains are diamonds that exhibit extraordinary constant sizes corresponding to ~1–2 nm. These data allow us to assume extremely complex and variable processes of mineral formation in stellar environments. In addition, it seems that the physical properties of minerals such as hardness have positively influenced the survival of especially diamonds throughout their long-term evolution.

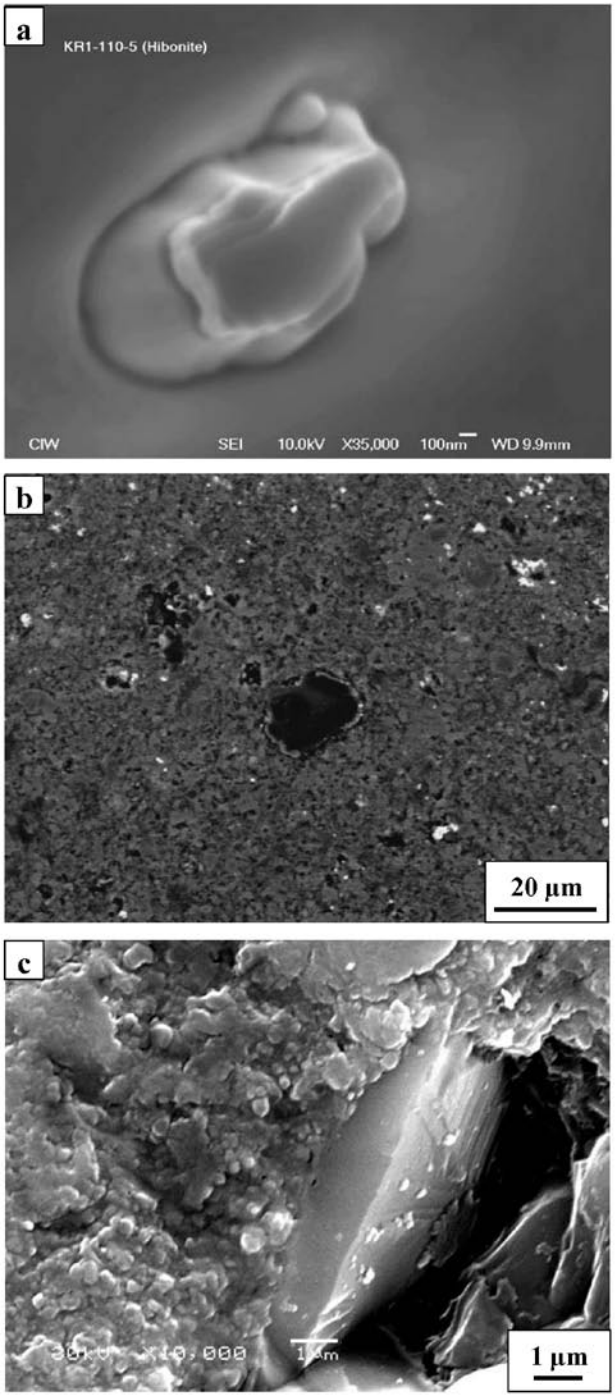

Because grain sizes of other presolar minerals vary by 1–2 orders of magnitude, we cannot rule out incorrect estimates of mineral abundances for the lowest size fractions. Chemical treatment of samples for isotope analysis includes a chemical separation of the grains that promotes their fragmentation. This must be considered an important factor when taking the increased fragility of meteoritic minerals compared with terrestrial analogs into account. For example, the size of a rounded grain of hibonite (Fig. 1b), found in situ within the fine-grained carbonaceous xenolith BK13 in Krymka (LL3.1) chondrite, corresponds to ≤ 20 × 10 μm (Semenenko et al., 2001), while the hibonite grains (Fig. 1a), chemically isolated from the same meteorite for isotope studies (Nittler et al., 2008) have fragmented shapes and sizes of ≤ 5.5 × 2 μm. Sizes of the chemically pretreated oxides including the hibonites found in other chondrites vary between 0.15–3 μm (Zinner, 2004). Thus, we suggest that the true size

Fig. 1. Condensate type fine grains in the Krymka chondrite. (a): SEM image of presolar hibonite, chemically isolated from the meteorite for isotope studies. The grain is located on a gold plate. The image is kindly provided by Larry Nittler. (b): BSE image of hibonite grain located in situ within the Krymka fine-grained carbonaceous xenolith BK 13 (Semenenko et al., 2001). A polished section of the meteorite. (c): BSE image of a complicated globular structure of fine-grained silicates and metal-sulfide intergrowths in the Krymka xenolith BK14. A face of the large olivine crystal contains nanometer-sized inclusions of chromite crystals (white). A broken surface of the chondrite polished section

ranges of all types of presolar minerals are unknown. However, very hard and physically strong phases like diamond and carbides may have survived significant grain fragmentation and miniaturization.

Some fine-grained portions of primitive meteorites composed of silicates, metal, and some accessory high-temperature minerals (Larimer, 1988) are probably relics of solar condensates (Brearley, 1996). Our scanning electron microscopic (SEM) examination of fractured surfaces of fine-grained xenoliths BK14 from Krymka, studied previously by V. Semenenko et al. (2001), and AL1 from Allende, show evidence for a complicated globular structure of silicates and metal-sulfide-intergrowths (Fig. 1c), i.e. individual globules are composed of many smaller globules. The smallest globules are less than 10 nm in diameter. Based on these data, an initial globular nucleation of minerals is suggested here followed by agglomeration (accretion) of globules within a dusty environment. From our point of view, namely the enhanced accretional property of nanometric grains (Gusev, 2009) favored the formation of the complex globules as well as the accretion of the fine-grained material. The existence of an amorphous state of the primary globules cannot be ruled out. Mild metamorphic conditions may have triggered crystallization at a later stage. This seems to be the most likely formation mechanism of the fine-grained condensates.

B. METAMORPHIC TYPE

Nanometer-sized minerals mainly present in pores, cracks, interfaces or within the mineral phases as inclusions are widely distributed in meteorites of different groups that have undergone thermal, shock or aqueous metamorphism. For example, the presence of many fine inclusions of silica (Fig. 2a), chromites, phosphides, phosphates or silicates, as shown by our SEM studies, is typical for nickel-iron and iron sulfides of shocked ordinary chondrites Galkiv (H4) and Gruz'ke (H4). Although much previously published work has been performed on this topic (e.g., Barber, 1981; Zanda et al., 1994; Brearley & Jones, 1998), we describe some new and genetically important examples of nanometer-sized mineral grains of metamorphic origin that we observed in meteorites.

One example shows a low-Ca pyroxene-rich microchondrule containing uniformly distributed nanocrystals of magnesium spinel with euhedral morphology (Fig. 2b). This unique microchondrule was found within a fine-grained rim of a porphyritic chondrule from Krymka with the aid of SEM and energy dispersive spectroscopic (EDS) studies. Based on mineralogy and chemistry, we suggest a high-temperature-event for the formation of the microchondrule. Most likely, it formed due to high-energy processes within a dusty environment. We further suggest that a slight metamorphism is responsible for the solid-state diffusion of Mg^{2+}, Al^{3+} and uniform nucleation of the tiny Mg-spinel crystals in the pyroxene-rich microchondrule.

We also observed rare nanometer- and micrometer-sized crystals of graphite, which are associated with organic compounds and other C-rich materials (Semenenko et al., 2004; Semenenko et al., 2005) of high scientific interest. Elucidation of their formation processes may also help to better understand the origin of terrestrial organic material and graphite deposits. The crystals observed in this study have a regular lamellar shape with sizes ≤ 3 x 0.7 μm and are uniformly dispersed throughout the fine-grained silicates of a carbonaceous xenolith from the Krymka chondrite (Fig. 2c). In most cases, the crystals are restricted to the interphase boundaries of minerals. According to transmission electron microscopic investigations (Weber et al., 2003), even small flakes of graphite with a thickness of less than 100 nm show a crystalline character. The occurrence of carbon within the carbonaceous xenoliths in three different forms (isolated crystals, organics, and C-rich material) suggests a genetic relationship of the graphite crystals with organic compounds. In accordance with Buseck and Bo-Jun (1985), the formation and ordering of the crystal structure of graphite is due to a mild thermal metamorphism of organics-containing material. The Krymka chondrite has been affected by significant shock metamorphism (Semenenko & Perron, 2005). We surmise that the metamorphic growth of graphite within the xenoliths was likely triggered by the collision of meteorite parent bodies in space. This conclusion is further corroborated by the enlargement of the graphite crystals, correlating with the degree of metamorphic processing of the xenolithic materials (Semenenko et al., 2004; Semenenko et al., 2005). The xenoliths represent a new kind of meteoritic component and some astrophysicists (e.g., Campins & Swindle, 1998) have speculated about a probable genetic relationship with mineral components of comets. Although the relationship between cometary and known meteoritic material is certainly an open question, a similar environment for the accretion of the xenolithic material in the protoplanetary disk and for comets cannot be excluded (Semenenko et al., 2005).

In the Knyahinya (L5) chondrite, some of the rare shock-melted structures observed can be best explained as high-temperature complexes of lyophilic emulsions composed of taenite and tiny, silicate-rich globules (Fig. 2d). The complicated structure and the extremely small size of the smallest globules indicate that the intensive shock was followed by high-temperature melting of metal and silicates, which nearly corresponds to a critical temperature of their mixing in some areas of the chondrite. Distinct shock features are also seen in the form of planar fractures and the start of weak mosaicism in olivines.

Unfortunately, we do not fully understand the formation processes of unique inclusions of native

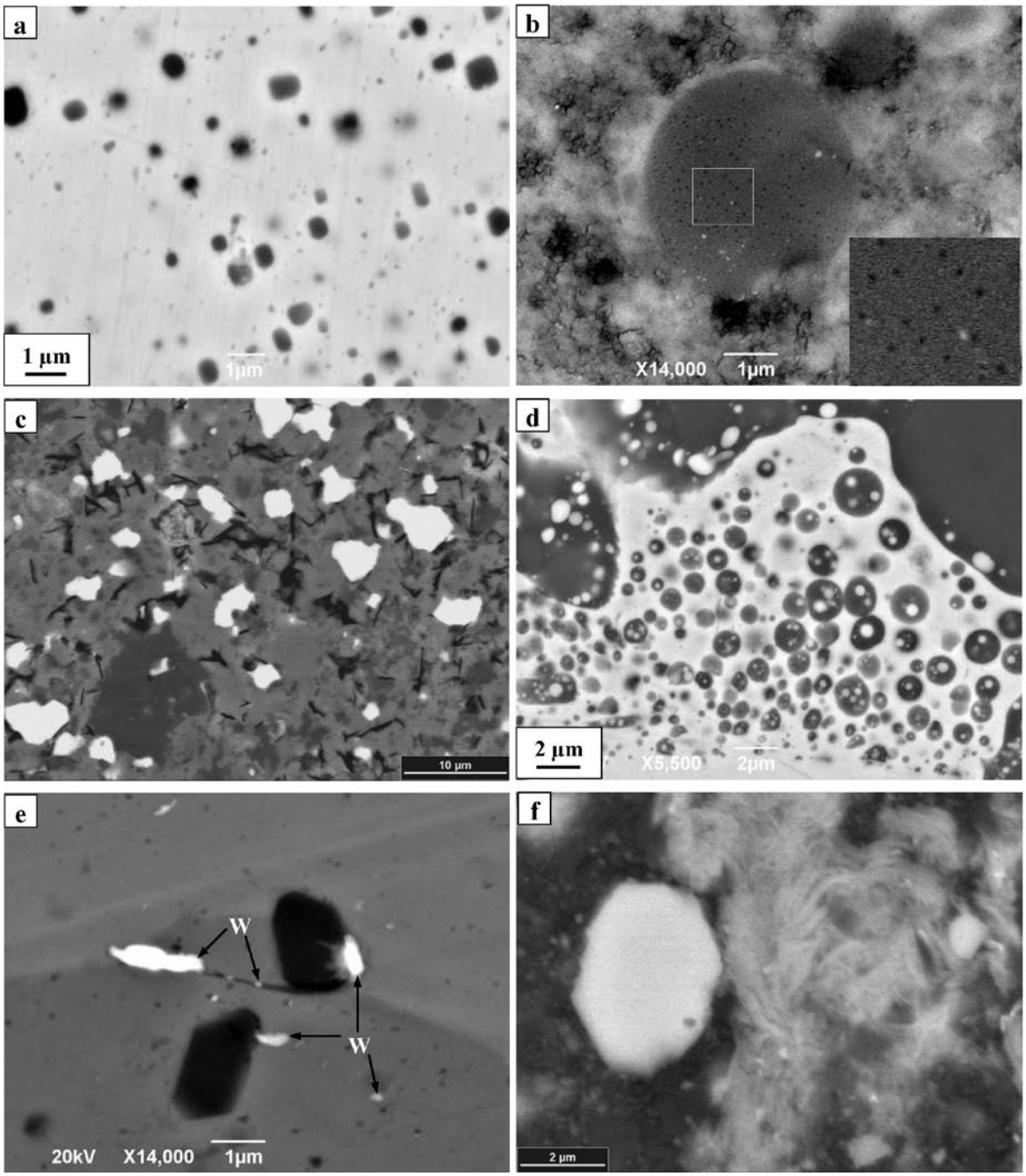

Fig. 2. BSE image of nanometer-sized grains of metamorphic type in polished sections of meteorites. (a): inclusions of silica (dark grey) within kamacite from the Galkiv (H4, shock stage S3) chondrite. (b): inclusions of spinel crystals in a low-Ca pyroxene-rich microchondrule embedded within fine-grained silicates from the Krymka chondrite. The enlarged part of the microchondrule with spinel (quadrangular black points) is presented in the right corner. (c): uniform distribution of graphite crystals (black) within the Krymka xenolith K1 (Semenenko et al., 2005). Silicates are light gray and gray, metal and sulfides are white. (d): lyophilic emulsion composed of taenite (white) and silicate-rich globules (gray) in the Knyahinya (L5) chondrite. (e): Unique inclusions of native tungsten (white) located within a kamacite globule (gray) found within a porphyritic chondrule from Krymka. Euhedral dark gray crystals are chromites. (f): Aggregates of fibrous crystals of phyllosilicates and magnetite crystals (white) within the Krymka fine-grained xenolith BK 1 (Girich & Semenenko, 2004).

tungsten (Fig. 2e) in the Krymka chondrite, which we found within a porphyritic chondrule with SEM and EDS study. Although W-bearing, refractory metal alloys are known from CAIs (MacPherson et al., 1988), to our knowledge, this is the first report of pure W-grains in meteorites. The inclusions are arranged within kamacite spherules embedded within the glass of a porphyritic chondrule, concentrated within cracks, pores and interfaces. The size of the smallest tungsten grain is ~50 nm. Their arrangement points towards a native origin. We do not consider these grains to be the result of contamination. The textural and mineralogical characteristics of the grains allow us to speculate on their formation process. The close connection between native tungsten and nickel iron indicates their genetic relationship. Although the very refractory grains of W condense at a higher temperature than nickel iron, we cannot exclude the following incorporation of W, for example, as nitrides or carbides, into nickel iron condensates. As high-temperature minerals, the W-bearing Fe,Ni-metals must have survived the melting process during chondrule formation. Later, stress-related shock metamorphism was probably favorable to the solid-state diffusion of W and formation of its inclusions within the kamacite cracks, pores and interfaces.

Aggregates of abundant cubic crystals of magnetite, i. e. framboids, as well as aggregates of fibrous crystals of phyllosilicates, comprise the most interesting secondary minerals that formed during low-temperature aqueous alteration of meteorite parent bodies (Zolensky & McSween, 1988). They occur in many CI and CM chondrites. These fibers within the Krymka fine-grained xenolith BK1 (Fig. 2f) are so thin (≤ 10 nm) that we were not able to obtain precise data on the chemical composition of these phyllosilicates (Girich & Semenenko, 2004). Microprobe analyses revealed that they contain Fe, Mg, Si, and minor amounts of S. It should also be mentioned that some fine-grained, water-bearing alteration products are regarded to be of pre-accretionary origin (Bischoff, 1998).

C. WEATHERING TYPE

Nanometer-sized secondary minerals that result generally from terrestrial weathering are widespread in meteorites. Our SEM and EDS studies show that different morphological types of iron hydroxide crystals occur mainly as clusters of globules, very thin fibers and needles (Fig. 3a-b), platelets of goethite or akaganeite (Fig. 3c). These dominate on surfaces of mineral grains of all types of weathered meteorites. Nanometer-sized hexagonal plates, likely of hematite, were observed in a few cases as oriented crystals on the surface of an olivine grain from the Omolon pallasite, probably along shear deformations (Fig. 3d). Laboratory monitoring of the weathering products in meteorite collections indicates that predominantly fibrous and lamellar nanocrystals with high surface energy are developed. Inasmuch as the nanocrystals are characterized by enhanced adsorptional properties (Gusev, 2009), this morphological feature of the secondary mineral grains promotes subsequent intensive degradation of meteoritic material.

Native silver belongs to one of the most interesting weathering products formed most likely in a terrestrial environment. It was found as separate fine grains (Fig. 3e) and dendritic-like agglomerates (Fig. 3f) in a polished section of the Krymka chondrite (Semenenko, 2010a, b). In most cases, the silver grains consist of nanoglobules with diameters ≤ 100 nm (Fig. 3f). They are located within Fe, Ni, S – hydroxides, which replace a remelted metal-troilite rim around a porphyritic olivine chondrule. According to energy dispersive data, the highest measured Ag content is 95.6 wt. %, where the other elements detected reflect contamination by the surrounding Fe, Ni, S – hydroxides. We also noted the presence of a few micrometric crystals of corundum adjacent to the silver grains.

Based on the tight association of the native silver with the Fe, Ni, S – hydroxides, its formation is most probably the result of weathering of hypothetic Ag-bearing metal-sulfides as is the case within the oxidation zones of terrestrial sulfides (Boyle, 1968; Latysh, 1997). This common process of terrestrial weathering includes two main stages: 1. transformation of Fe^0 and Fe^{2+} to Fe^{3+}, 2. solid-state diffusion of Ag and formation of native silver inclusions within the hydroxides due to the discrepancy of its atomic radius with the ionic radius of Fe^{3+}. The data allow us to speculate on a possible condensation origin of Ag-bearing pristine minerals. We suppose that nickel iron and/or iron sulfides (Palme et al., 1988), accreted to the chondrule surface from a dusty environment. In light of the fact that presolar corundum has been chemically separated from Krymka and isotopically characterized (Nittler et al., 2008), the presolar nature of both the corundum crystals and an Ag-bearing precursor of the extremely rare grains of native silver is not excluded (Semenenko, 2010a, b).

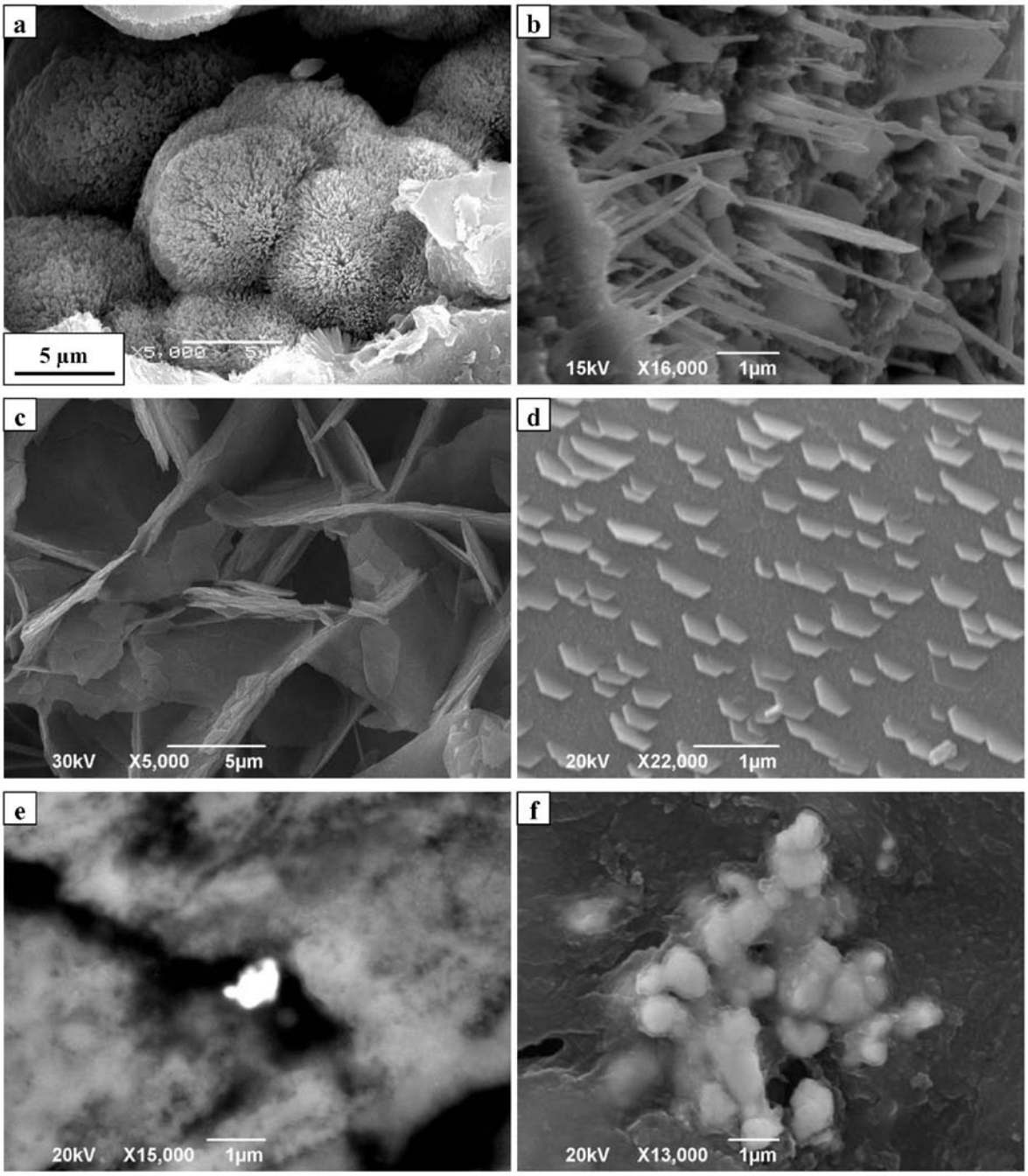

Fig. 3. SE and BSE (e) images of nanometer-sized grains of weathered type on fractured surfaces and in polished sections (e, f) of meteorites. (a, b): fine, fibrous needles of goethite within the ungrouped ataxite Chinga (a) and in the Galkiv chondrite (b). (c): very thin platelets of iron hydroxides with ~15 wt. % NiO arranged on a surface of the intensively weathered Berdyansk (L6) chondrite. (d): hexagonal plates, likely hematite, probably located along shear deformations on the surface of an olivine grain from the pallasite Omolon. (e): Separate grain of native silver in the Krymka meteorite. The grain is located within a crack in Fe,Ni,S-hydroxides belonging to weathering products of metal-troilite. (f): complicated globular structure of an agglomerate of native silver within iron hydroxides of the Krymka meteorite

CONCLUSIONS

1. Nanometer-sized mineral grains are ordinary constituents of all types of meteorites. Most of them occur within the fine-grained silicate material of primitive meteorites.

2. Complicated globular morphology is typical for condensing nanometer-sized grains, whereas fibrous or lamellar morphology is common for weathering products.

3. Enhanced accretional properties of nanometer-sized grains could be responsible for the accretion of primary condensed nanoglobules within a protoplanetary nebula.

4. Morphological features of weathered products promote subsequent intensive degradation of meteoritic material due to their enhanced adsorptional properties.

5. Only the primitive meteorites contain different genetic types of nanometer-sized grains that resulted from the structural ordering of solid matter as a fundamental process in the formation of minerals in stellar, nebular or solid bodies environments.

ACKNOWLEDGMENTS

We are sincerely grateful to Larry Nittler for kindly providing the SEM image of the Krymka presolar hibonite and to Addi Bischoff and Ulrich Ott for the correction out English and many helpful and constructive advices.

REFERENCES

Barber D.J., 1981 – Matrix phyllosilicates and associated minerals in C2M carbonaceous chondrites. *Geochimica et Cosmochimica Acta*, 45, 945-970.

Bischoff A., 1998 – Aqueous alteration of carbonaceous chondrites: Evidence for preaccretionary alteration – a review. *Meteoritics & Planetary Science,* 33, 1113–1122.

Bischoff A., Vogel N., Roszjar J., 2011 – The Rumuruti chondrite group – Invited Review. *Chemie der Erde – Geochemistry,* 71, 101–134.

Boyle R.W., 1968 – The geochemistry of silver and its deposits. *Bull. Geol. Surv. Can*., 160 (6), 264.

Brearley A.J., 1996 – Nature of matrix in unequilibrated chondrites and its possible relationship to chondrules. In: *Chondrules and the Protoplanetary Disk* (eds. Hewins R. H. et al.). Cambridge University Press, New York, 137–151.

Brearley A.J., Jones R.H., 1998 – Chondritic meteorites. In: *Planetary Materials, Reviews in Mineralogy* (ed. Papike J. J.). Mineralogical Society of America, Washington, DC, Vol. 36, 313–398.

Bukanov V.V., 2001 – *Colored stones. Gemological dictionary*. Publishers "Bronze Horseman", St. Petersburg, 208 (in Russian).

Buseck P.R., Bo-Jun H., 1985 – Conversion of carbonaceous material to graphite during metamorphism. *Geochimica et Cosmochimica Acta*, 49 (10), 2003–2016.

Campins H., Swindle T.D., 1998 – Expected characteristics of cometary meteorites. *Meteoritics & Planetary Science*, 33 (6), 1201–1211.

Girich A.L., Semenenko V.P., 2004 – Mineralogy of magnetite-bearing xenoliths in the Krymka (LL3.1) stone meteorite. *Reports of the National Academy of Sciences of Ukraine*, (9), 105–113 (in Ukrainian).

Gusev A.I., 2009 – Nanomaterials, nanostructures, nanotechnology. Publishers "Physmatlit", Moscow, 416 (in Russian).

Larimer J.W., 1988 – The cosmochemical classification of the elements. In: *Meteorites and the early Solar system* (Eds. Kerridge J. F., Matthews M. S.). The University of Arizona press, Tucson, 375–389.

Latysh I.K., 1997 – Silver in nature. Publishers "Artek", Kiev, 134 (in Russian).

Lodders K., Amari S., 2005 – Presolar grains from meteorites: Remnants from the early times of the solar system. *Chemie der Erde*, 65 (2), 93–166.

MacPherson G.J., Wark D.A., Armstrong J.T., 1988 – Primitive materials surviving in chondrites: refractory inclusions. In: *Meteorites and the early Solar system* (Eds. Kerridge J. F., Matthews M. S.). The University of Arizona press, Tucson, 746–807.

Nittler L.R., Alexander C.M.O'D, Gallino R., Hoppe P., Nguyen A.N., Stadermann F.J., Zinner E.K., 2008 – Aluminum-calcium- and titanium-rich oxide stardust in ordinary chondrite meteorites. *The Astrophysical Journal*, 682 (2), 1450–1478.

Palme H., Larimer J.W., Lipschutz M.E., 1988 – Moderately volatile elements. In: *Meteorites and the early Solar system* (Eds. Kerridge J. F., Matthews M. S.). The University of Arizona press, Tucson, 436–461.

Semenenko V.P., 2010a – Native silver in a meteorite. *Meteoritics & Planetary Science*, Supplement, 45, A187.

Semenenko V.P., 2010b – First found of native silver in meteorites. *Proceedings of Ukrainian Mineralogical Society*, 7, 58–63 (in Ukrainian).

Semenenko V.P., Perron C., 2005 – Shock-melted material in the Krymka LL3.1 chondrite: Behavior of the opaque minerals. *Meteoritics & Planetary Science*, 40 (2), 173–185.

Semenenko V.P., Bischoff A., Weber I., Perron C., Girich A.L., 2001 – Mineralogy of fine-grained material in the Krymka (LL3.1) chondrite. *Meteoritics & Planetary Science*, 36 (8), 1067–1085.

Semenenko V.P., Girich A.L., Nittler L.R., 2004 – An exotic kind of cosmic material: Graphite-containing xenoliths from the Krymka (LL3.1) chondrite. *Geochimica et Cosmochimica Acta,* 68 (3), 455–475.

Semenenko V.P., Jessberger E.K., Chaussidon M., Weber I., Stephan T., Wies C., 2005 – Carbonaceous xenoliths in the Krymka LL3.1 chondrite: Mysteries and established facts. *Geochimica et Cosmochimica Acta*, 69 (8), 2165–2182.

Semenenko V.P., Girich A.L., Shyrinbekova S.N., Gorovenko T.N., 2010 – Genetical types of nanometric mineral grains in meteorites. *Thesis of reports on international scientific conference "Nanostructural materials – 2010: Byelorussia – Russia – Ukraine"*, Kyiv, 183 (in Russian).

Weber I., Semenenko V.P., Stephan T., Jessberger E.K., 2003 – TEM investigation of a "mysterite" inclusion from the Krymka LL-chondrite: Preliminary results. *Lunar and Planet. Sci.*, 34, 1535.

Zanda B., Bourot-Denise M., Perron C., Hewins R.H., 1994 – Origin and metamorphic redistribution of silicon, chromium, and phosphorus in the metal of chondrites. *Science*, 265 (9), 1846-1849. 17–39.

Zolensky M., McSween H.Y.Jr., 1988 – Aqueous alteration. [In:] *Meteorites and the early Solar system* (Eds. Kerridge J. F., Matthews M. S.). The University of Arizona press, Tucson, 114–143.

Zinner E.K., 2004 – Presolar grains. [In:] Davis A.M., Holland H.D. (Eds), *Treatise on Geochemistry. Meteorites, Comets and Planets*. Elsevier, Pergamon Press, Vol. 1, pp. 17–40.

Publishers: Wrocław University of Technology, Faculty of Geoengineering, Mining and Geology
Polish Meteorite Society

Meteorites
Vol. 1, No. 1, 2011, 21–28
www.meteorites.pwr.wroc.pl
DOI 10.5277/met110103

NEW FINDS IN THE MORASKO METEORITE PRESERVE, POLAND

Łukasz KARWOWSKI[1], Andrzej S. PILSKI[2], Andrzej MUSZYŃSKI[3], Steve ARNOLD[4], Geoffrey NOTKIN[5], Agnieszka GURDZIEL[1]

[1] University of Silesia, Faculty of Earth Sciences, ul. Będzińska 60, 41-200 Sosnowiec, Poland.
[2] Nicolaus Copernicus Museum, ul. Katedralna 8, 14-530 Frombork, Poland.
[3] Adam Mickiewicz University, Institute of Geology, ul. Maków Polnych 16, 60-606 Poznań, Poland.
[4] Meteorite Men Headquartes, P.O.Box 36652 Tucson, AZ 85740, USA.
[5] Aerolite Meteorites LLC, P.O.Box 36652 Tucson, AZ 85740, USA.

Abstract: In result of searching in the Morasko preserve for the documentary series *Meteorite Men* two irons were found below ground. A 544-g shrapnel-like with weak shock deformations, mildly weathered, at low depth, and 34-kg individual, with its upper surface 156 cm deep, with a thick shell of clay and weathering minerals. Of particular interest is presence of chukanovite, a mineral discovered in the Dronino iron meteorite. Morasko is the second meteorite, where chukanovite could be found.

The recovery of a new specimen so much deeper than the previous depth record, suggests that further, more detailed surveys should be conducted in the future with improved metal detecting equipment. Moreover, the larger specimen was found embedded in a Miocene clay, which demonstrates that it fell from the sky at that exact spot and was not deposited in glacial terminal moraine.

Keywords: iron meteorite Morasko, new finds, strewnfield

INTRODUCTION

The Morasko iron meteorite has been known since 1914, when a mass of iron, 77.5 kg, was found while digging trenches at the town of Morasko near the Poznan city (Grady, 2000). Later a few more irons were recovered, and in late 1950 Jerzy Pokrzywnicki found evidence of multiple fall in Morasko, and noticed eight pits that could be meteorite craters (Pokrzywnicki, 1964). His efforts resulted in the formation of the Morasko meteorite preserve in 1976 in order to protect the area around the craters.

In the 1970s, research on Morasko was continued under direction of Hieronim Hurnik from Adam Mickiewicz University and resulted in publications on the strewnfield, and composition of the meteorite (Hurnik, 1976; Dominik, 1976).

In the last two decades, access to better equipment resulted in the recovery of hundreds of iron meteorites by private meteorite hunters in the fields and forests mostly north and east of the craters, and outside of the protected area. At the same time, comprehensive research in the Morasko area were made by scientists and students of the Geological Institute of Adam Mickiewicz University in Poznań (Stankowski, 2001). In 2005 the University was granted permission to search for meteorites in the Morasko preserve over a two-year period (permission SR.III-2.6630-89/04/05). The search was conducted on behalf of the university by Krzysztof Socha, an experienced meteorite hunter who had previously found hundreds of Morasko irons outside the preserve. As a result, 13 meteorites larger than 1 kg were found, including the largest specimen ever recovered (164 kg after cleaning), plus many smaller irons (Muszyński et al., 2007). Because of snow or dense vegetation searching

Corresponding author: Andrzej S. PILSKI, aspmet@wp.pl
[1] Permission SR.III-2.6630-89/04/05

was only possible during early spring and late autumn. Moreover, the preserve was full of scrap iron and lead bullets, which made working with metal detectors slow and laborious. As the result of these obstacles, the two-year season turned out to be too short, and part of the preserve area was left unsearched.

The results of research on the Morasko iron were summarized by Wojciech Stankowski (2008). After a few reclassifications the Morasko iron was finally classified as IAB-MG (Wasson & Kallemeyn, 2002).

An opportunity to continue searching presented itself in 2011, when Discovery Science and LMNO Cable Productions applied for permission to film an episode of the documentary series, *Meteorite Men,* at Morasko. As part of a joint research project with Adam Mickiewicz University, the permission – WPN-II.6205.43.2011.MM – was given for a five-week season that would include searching and filming. Due to the limitations of participants, searching was done in two short periods: June 28–29 and July 18–21, 2011.

METHODS

Two metal detectors were used in the search: a hand detector, which employed VLF (very low frequency) technology and another hand detector, which employed the pulse induction (PI) technology, with an 18-inch coil, which was replaced during the second search season with a 2-meter coil for deeper targets.

Finds were ground or cut to unveil metal and then the metal surfaces were etched with nital.

Loose clay was cleaned off from the second specimen, and part of the weathering crust was removed for analyses. Then an end piece was cut and etched for examination under an optical microscope, and another slice was cut and prepared for analysis. Mineral phases were investigated using a scanning electron microscope equipped with EDS (EDAX) detector and an X-ray diffractometer X'Pert Philips PW 3710 at the Faculty of Earth Sciences, University of Silesia and an electron microprobe CAMECA SX 100 at the Faculty of Geology, Warsaw University.

FINDS

The northwestern part of the preserve was chosen to begin the search, an area that had not been extensively covered by Krzysztof Socha. From among many iron fragments found, two pieces were proven to be real meteorites. The first meteorite was found on July 29 by Andrzej Pilski (Fig. 1). A 544-g piece of iron with a thin weathered crust, it was found about 30 cm below ground, among stones of similar size or larger, with sand between them. The find was cut in half and etched. Its etched surface shows an irregular, coarse Widmanstätten pattern with Neumann lines in kamacite (Fig. 2). Both the Widmanstätten pattern and Neumann lines are distorted in places because of shock influence. There are no larger inclusions visible. Schreibersite appears in form of rhabdite, and in some places between kamacite bars replacing taenite.

The second meteorite was located on July 19 by Steve Arnold using a PI detector with a 2-meter coil. Because of its great depth, and without the ability to use mechanical devices for excavation, the iron could

Fig. 1. The 544 g iron found on June 29, 2011 in the Morasko preserve

Fig. 2. Etched cross section of the 544 g find

Fig. 3. The 34 kg Morasko iron seen from two sides. Dimentions: 28 × 24 × 18 cm. It is shown upside down relative to its position in the clay.

only be uncovered at the end of next day. Its upper surface was 156 cm below ground, buried in the colorful Poznan clay (Miocene in age). After preliminary cleaning its weight was determined to be 34 kg, and size 28×24×18 cm. Despite cleaning the iron was still covered with clay tightly attached to the meteorite itself.

During examination, an attempt was made to first remove the attached clay and unveil crust or metal. The result was a large end piece of totally weathered rock that was chipped out, plus a few other fragments of minerals from the weathering crust. It was discovered that the lump of iron was deeply weathered and it was hard to uncover clean metal. In order to determine the depth of the weathering crust, a larger end piece was cut. After cutting and etching the cut surface, it was found that weathering was irregular. Some areas were deeply affected and in other places nickel iron alloy was intact even at shallow depths (Fig. 5).

PETROGRAPHY AND MINERALOGY OF THE LARGE FIND

On the meteorite cross section two different areas are clearly visible. About one half of it (lower on Fig. 5) is rich in cohenite, grains of which mimic the Widmanstätten pattern, and being situated between kamacite

Fig. 4. Deeply weathered section after removing an end piece from the upper right side on Fig. 3, left.

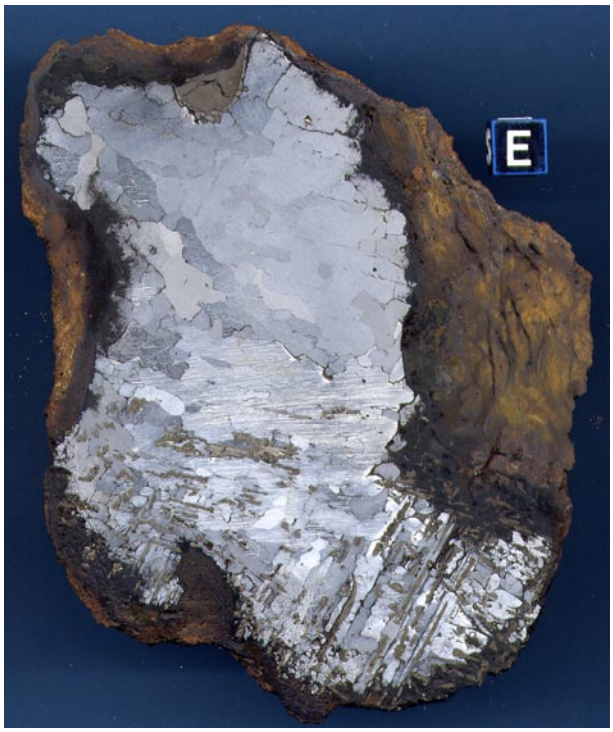

Fig. 5. Etched cross section of the 34 kg find. There are many cohenite inclusions in the lower part and two elongated, horizontal schreibersite inclusions below center; the lower one is rimmed with cohenite. Part of a troilite inclusion rimmed with schreibersite is seen at the upper edge

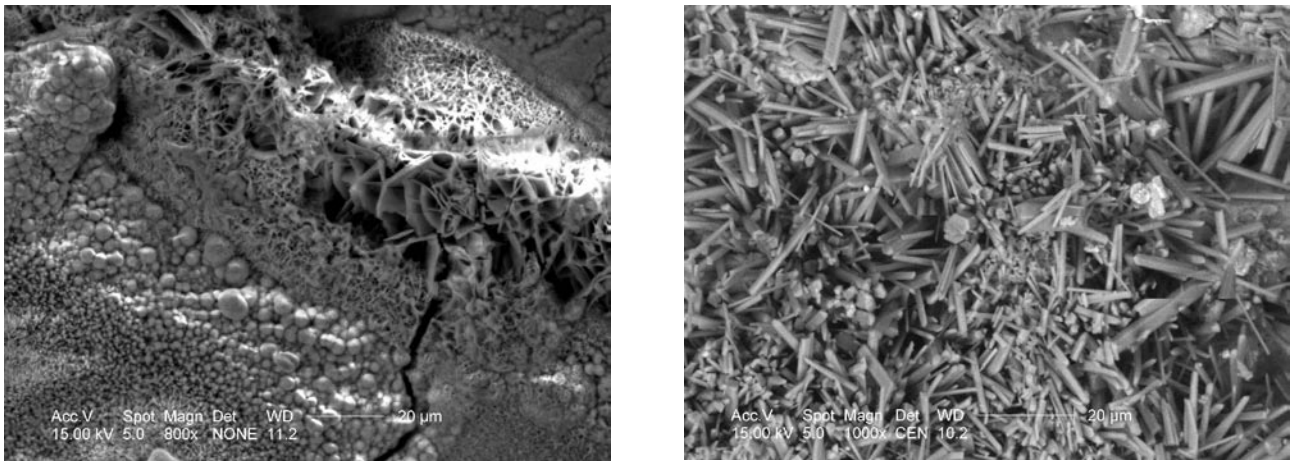

Fig. 6. Minerals in the external layer. Left: iron hydroxides. Right: a druse of aragonite. SEM image

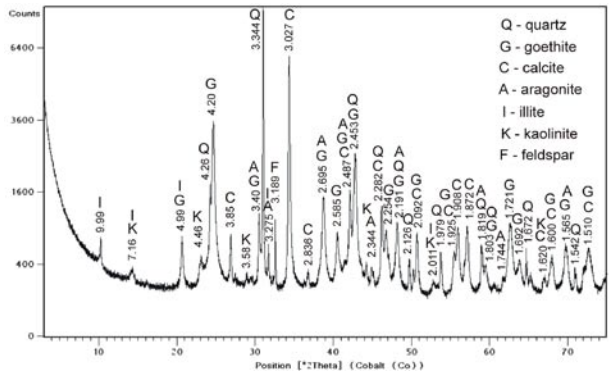

Fig. 7. X-ray diffraction pattern of minerals in the most external part of weathering crust

plates or inside them. The cohenite pattern continues into a deeply weathered area (lower right on Fig. 5), where the kamacite is completely weathered out into hydroxides, but cohenite seems to be intact. The second half (upper on Fig. 5) is cohenite-free and texturally resembles the first iron find, except there are no signs of shock influence. Generally the unweathered part of the specimen seems to be typical of Morasko, the petrology of which was described in detail by B. Dominik (1976), Karwowski & Muszyński (2008), Karwowski et al. (2009).

The most external layer of the meteorite is not its real weathered section, but the attached clay, cemented with some iron oxides. In the case of our specimen the cementing mineral is goethite. Its origin is debatable, but most likely the iron in goethite is a result of clay coming in contact with the meteorite. Usually an iron meteorite will act as a strong reducing agent and attract iron and manganese from its surroundings. Goethite is associated with calcite and aragonite; the last mentioned often forms tiny druses within the crust (Fig. 6). The cemented material comprises of small grains of quartz, muscovite, kaolinite with some addition of feldspar (Fig. 7). It seems that the meteorite, when penetrating the clay, some surface material (soil) adhered to its front.

The weathered meteorite forms the next layer beginning with a relatively homogenous layer of iron

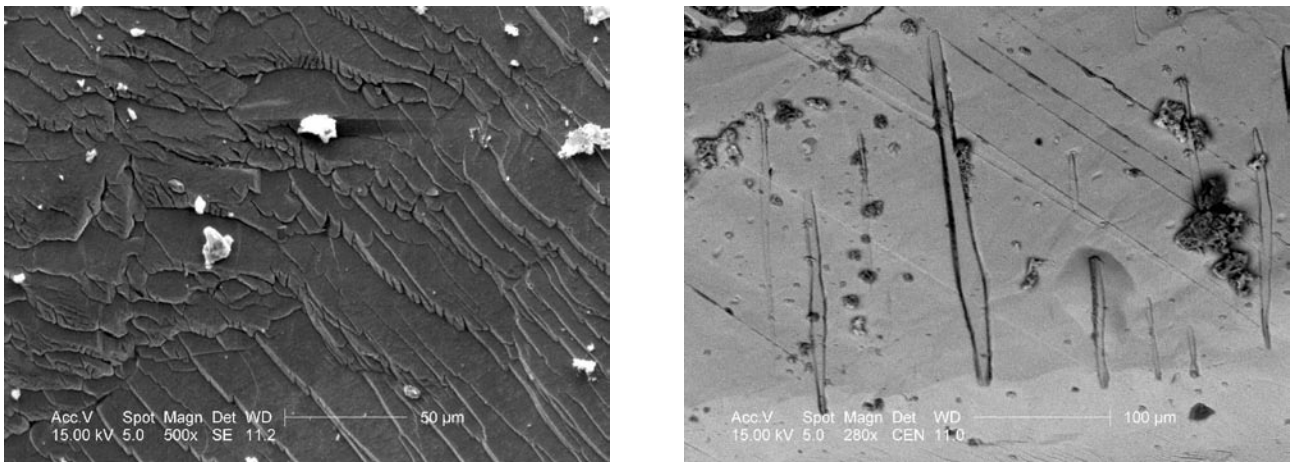

Fig. 8. Taenite. Left: surface with growth steps. Right: elongated exsolutions of nickelsulphide on the surface of a taenite lamelle. SEM image

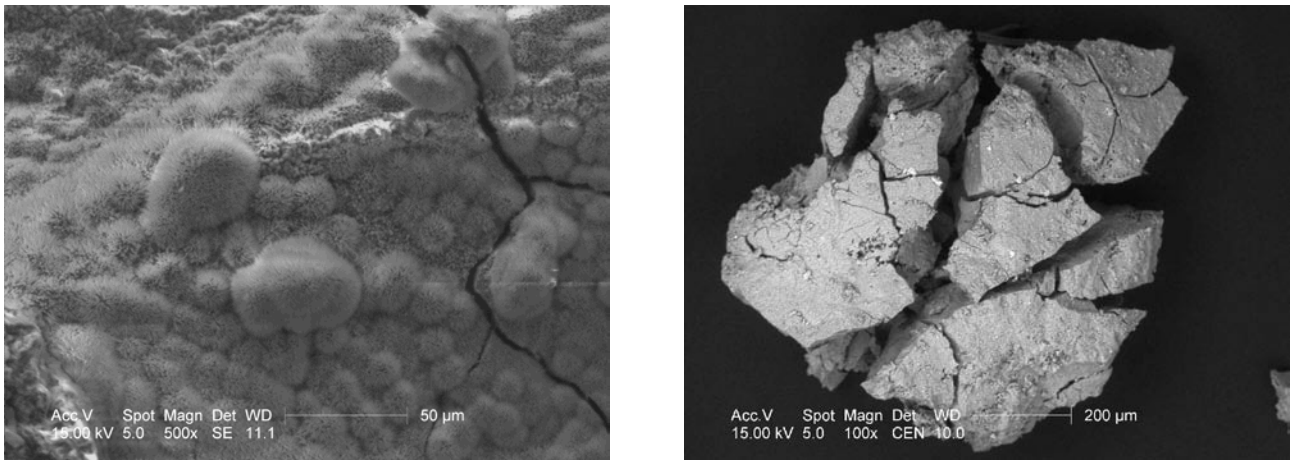

Fig. 9. Left: a microdruse of chukanovite. Right: a desintegrating grain of helleyrite. SEM image

hydroxide, mainly goethite, with lepidocrockite in places. After cutting and polishing, the layer shows conspicuous luster. The next layer contains tiny metal phases, represented mainly by taenite in the form of thin plates with distinct surfaces (Fig. 8). In some places elongated grains of nickelphosphide are attached to taenite plates.

Spaces between taenite plates are filled with hydroxides and carbonates together with aggregates of an emerald-green substance. In some places there is a dark gray substance with romboedric cleavage. After a detailed examination it was found that it is the pseudomorph after kamacite and its cleavage comes from Neumann lines. The substance is composed mainly of chukanovite (Fig. 10) with minor taenite and small addition of siderite, where some Fe is replaced by Ca and Mg. These elements were probably absorbed from outside with carbon dioxide. In some places small microdruses of green chukanovite can be seen.

Additionally, small amounts of goethite and hellyerite ($NiCO_3.6H_2O$) could be seen. The last mineral is emerald-green and unstable. In a laboratory it disintegrates quickly into an amorphous, greenish mass. Hellyerite was discovered on SEM images and its presence was confirmed with EDS analysis.

In the unweathered, internal section of the meteorite, the cohenite zone ends with a conspicuous, elongated inclusion of schreibersite rimmed with cohenite. A nearby, elongated schreibersite inclusion with no cohenite rim, is the beginning of the cohenite-free zone. There can be seen a schreibersite inclusion inside the kamacite crystal, some elongated schreibersite inclusions replacing taenite between kamacite plates, and a schreibersite rim around the troilite inclusion on edge, which continues into the weathered part.

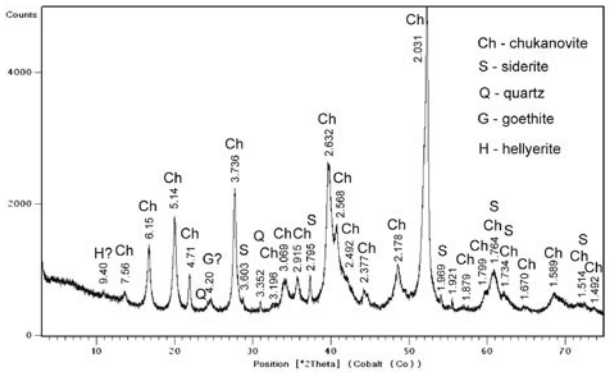

Fig. 10. X-ray diffraction pattern of chukanovite

DISCUSSION

The search was very limited, due to time constraints. Sampling was carried out in different areas, but unfortunately neither a survey of the entire area, nor a controlled exhaustive in very defined areas could be completed.

A comparison of both finds confirms once again that the weathering grade may depend more on terrestrial environment than on the terrestrial age of a meteorite. The smaller specimen was found in a slightly elevated place, cut with trenches, among stones, where water had no chance to accumulate for any length of time. The larger meteorite was found in the clay, which can retain water for long time, as was demonstrated when rain fell during the excavation. As both

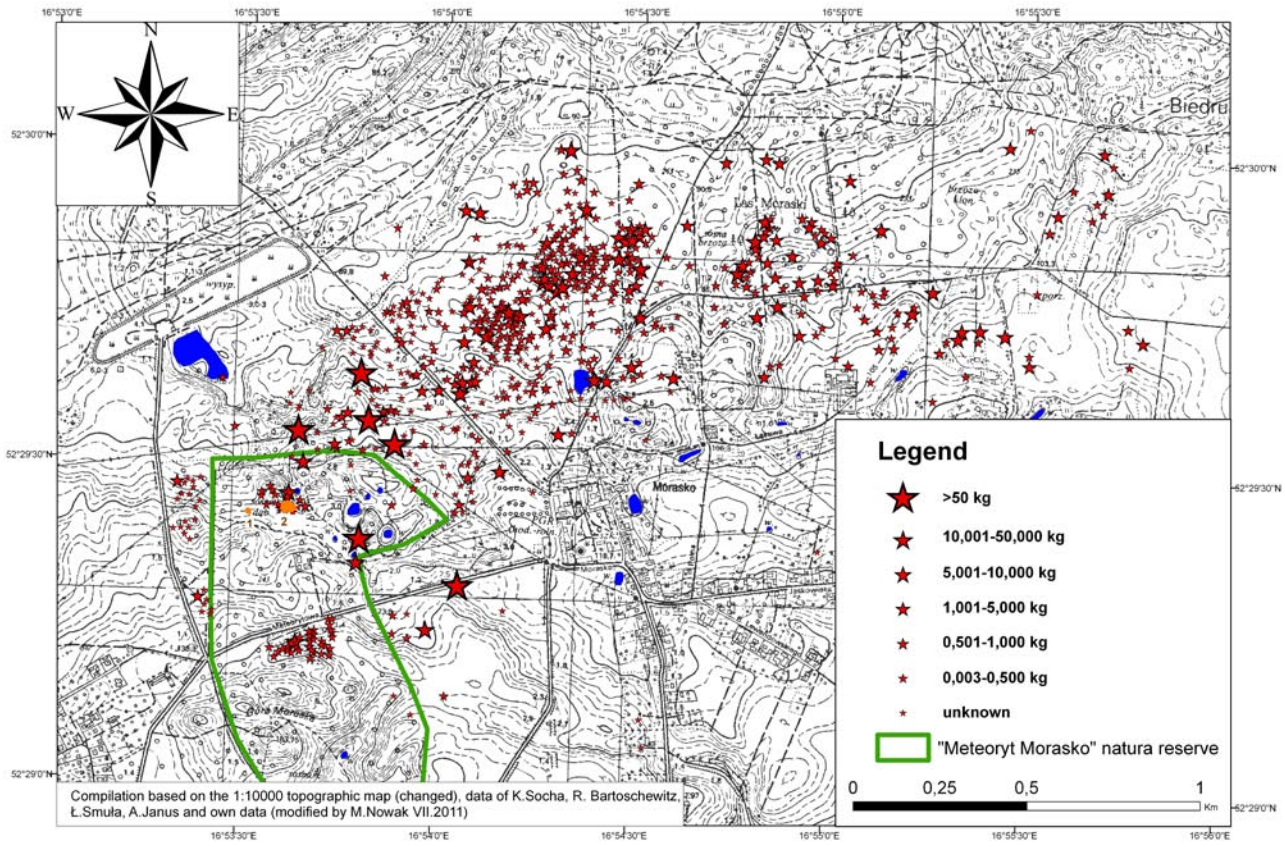

Fig. 11. The orange spots mark locations of the new finds: 1 = 544 g and 2 = 34 kg. Map from Muszyński et al., 2012

finds belong to the same meteorite shower, their terrestrial age is the same, but their weathering grades are entirely different.

Characteristic of the Morasko strewnfield are numerous finds confined to relatively small area on the northern slope of a terminal moraine. This gave reason to a supposition, that possibly meteorites showered onto a glacier during the most recent period of glaciation, and then they were transported by the glacier and deposited in terminal moraine. If this is correct, all meteorites should be found in relatively shallow depths and in strata deposited during the last glaciation. Until now all finds were buried at relatively shallow depths suggesting that this supposition may be accurate. The 34-kg find, embedded in the Poznan clay with an age of more than 5 million years, obviously had to penetrate the clay rather than being deposited. It seems the only reason for relatively shallow finds is that less sensitive detectors were unable to locate the deeply-buried irons.

A characteristic of the external layer of the 34-kg specimen is the presence of substantial amounts of carbonates. The outer part of the meteorite coating consists of relatively light colors, and contains kaolinite, minerals from the mica group, both light and dark, goethite, quartz as well as aragonite and calcite. The presence of aragonite clearly distinguishes this find from Morasko specimens that were found at shallower depths. In those specimens calcium carbonates were rare and sometimes only occurred on the bottom faces of meteorites, due to the crystallization of oozing solutions from moraine formations. They only appeared in the form of calcite. In the analyzed find aragonite clearly dominates and it forms tiny druses on the sides of cracks. Most often aragonite crystals form distinctive triplets of pseudohexagonal morphology (Fig. 6, right).

Another distinctive feature that makes the specimen under consideration of particular interest, is the presence of chukanovite ($Fe_2(CO_3)(OH)_2$) as a dominant mineral phase in pseudomorphs after kamacite with distinctive quasi-cleavage as a relic after Neumann lines in kamacite, as well as the presence of emerald-green, unstable in room conditions, hellyerite ($NiCO_3 \cdot 6H_2O$). The authors are of the opinion that the presence of chukanovite and hellyerite is a result of a specific stability of climatic conditions (temperature, constant humidity, limited accessibility of oxygen) existing at a depth of 1.5–2 meters below the ground in this region.

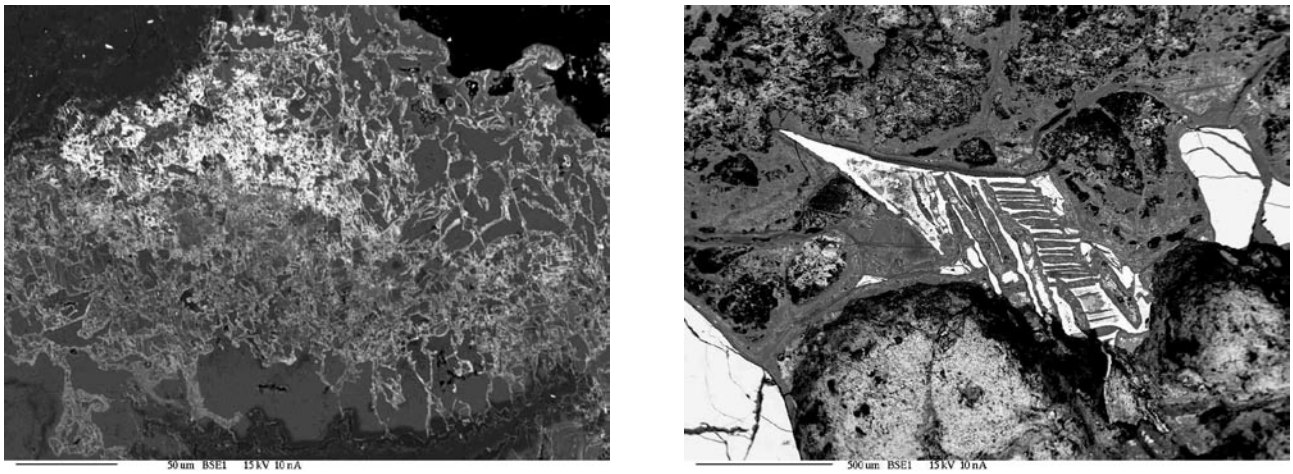

Fig. 12. Left: nickel exsolutions. Right: weathering of taenite. BSE images

Weathering acted most quickly on metal phases: mainly kamacite and to a lesser extent, taenite and tetrataenite. Kamacite was nearly completely transformed into a mixture of chukanovite and iron hydroxides. Inside this mixture tiny druses appeared, filled with greenish needles of chukanovite or, less often, with dripstones of clear, colorless iron hydroxides (Fig. 6, left), which quickly turned yellow (a rusty color), and became turbid and dehydrated. In the most external layers of the meteorite only iron hydroxides – mainly goethite – could be seen.

Weathering resulted in the separation of nickel from iron. Nickel is concentrated among secondary carbonates and hydroxides as a separate mineral phase of native nickel (Fig. 12, left). The secondary exhalations of nickel are enriched with germanium and, in the analyzed specimen, they contained up to 2.56 wt% Ge, which means a 60-times enrichment relative to typical Ge content in Morasko meteorites. The highest Ge contents appear in the most external appearances of the secondary Ni. A still higher Ge content in the secondary Ni metal was measured by Karwowski & Gurdziel (2009).

Weathering of taenite depends upon nickel content (Fig. 12 right), and low-Ni phases are destroyed first. The most resistant are high-Ni phases and tetrataenite. In the most external layers of a weathering iron meteorite only relics of tetrataenite may be seen (Fig. 13). The minerals most resistant to weathering are schreibersite and nickel phosphide. Characteristic of schreibersite inclusions in the specimen under consideration is a high Ni content: nearly 1:1 relative to Fe content, whereas the nickelphosphide contains more nickel, from 39.78 to 42.31 at% of Ni. These phases seem not to be affected by secondary processes.

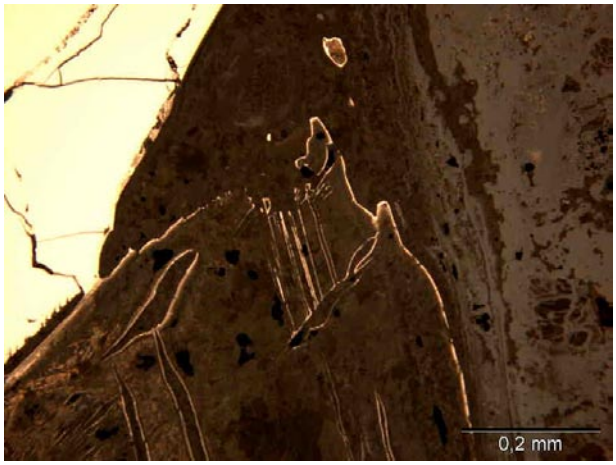

Fig. 13. Tetrataenite left after taenite totally weathered out. BSE image

Slightly less resistant is cohenite, in which iron hydroxides grow along cracks. Low-Ni kamacite from a cohenite decomposition and secondary graphite were not observed.

Cleaning finds and removing dirt and rust crust to expose metal or at least a crust on the metal is a common practice among iron meteorite hunters. This can result in the removal of all weathering minerals before a meteorite is examined by scientists. Due to a different approach with the larger find, a rare mineral, chukanovite, was discovered first time in Morasko specimens and only the second time in any meteorite, the first being the iron meteorite Dronino (Pekov et al., 2007). As the 34-kg find is not the first Morasko specimen to be so highly weathered, it seems possible that the mineral could have been detected earlier if other finds were not so thoroughly cleaned.

CONCLUSIONS

Applying new detecting techniques to the Morasko strewnfield resulted in the discovery of a Morasko specimen with its upper surface buried 156 cm below the ground, deeper than any previous Morasko find. It seems possible that more irons exist that could not be located until now because detectors were not sensitive enough to locate deeply-buried specimens. More detailed surveys should be conducted in the future with the improved equipment available today.

These new finds confirm, once again, that weathering grade is a poor indicator of the terrestrial age of an iron meteorite and depends mainly on conditions in the soil around a meteorite specimen. Moreover, composition of the soil is an important factor that helps determine both the type and the rate of weathering.

The find of the 34-kg Morasko specimen in Poznan clay is evidence that the Morasko meteorites fell in situ and were not transported by glaciers. The idea that the meteorites might have been deposited by glacier on the terminal moraine "Moraska Góra" has been proven incorrect.

REFERENCES

Dominik B., 1976 – Mineralogical and chemical study of the coarse octahedrite Morasko. *Prace Mineralogiczne PAN,* 47, 7–53 (in Polish).

Grady M.M., 2000 – Catalogue of Meteorites, 5th edition. Cambridge University Press, Cambridge, UK.

Hurnik H. (Ed), 1976 – Meteorite „Morasko" and the region of the fall of the meteorite. Adam Mickiewicz University (Poznań), Astronomia 2, 64.

Karwowski Ł., Gurdziel A., 2009 – Secondary minerals in Morasko and Pułtusk meteorites. *Vestnik Lviv. Univ. Ser. Physics. 2009.* 43, 243–248.

Karwowski Ł., Muszyński A., 2008 – Multimineral inclusions in the Morasko coarse octahedrite. *Meteoritics* & *Planetary Science,* 43, A71.

Karwowski Ł., Muszyński A., Kryza R., Helios K., 2009 – Phosphates in the Morasko meteorite. *Mineralogy – Special Papers*, 35, 90–91.

Karwowski Ł., Muszyński A., Kryza R., Pilski A.S., 2009 – Polimineralne nodule w gruboziarnistym meteorycie Morasko. *Acta Societas Metheoriticae Polonorum,* 1, 52–58 (in Polish).

Muszyński A., Bartoschewitz R., Pilski A.S., Kryza R., 2012 – The Morasko strewnfield and its possible extension to a few more iron finds (in preparation).

Muszyński A., Pilski A.S., Socha K., 2007 – Two Years in the Morasko Reservation, *Meteorite*, 13 (4), 10–12.

Pekov I.V., Perchiazzi N., Merlino S., Kalachev V.N., Merlini M., Zadov A.E., 2007 – Chukanovite, $Fe_2(CO_3)(OH)_2$, a new mineral from the weathered iron meteorite Dronino. *European Journal of Mineralogy*, 19 (6), 891–898.

Pokrzywnicki J., 1964 – Meteorites of Poland. *Studia Geologica Polonica*, Vol. 15, 176 (in Polish).

Stankowski W., 2008 – Morasko meteorite a curiosity of the Poznań region. Time and results of the fall. Adam Mickiewicz Press, Seria geologia, 19, 91.

Stankowski W.T.J., 2001 – The geology and morphology of the natural reserve „Meteoryt Morasko". *Planetary and Space Science*, 49, 749–753.

Wasson J.T., Kallemeyn G.W., 2002 – The IAB iron-meteorite complex: A group, five subgroups, numerous grouplets, closely related, mainly formed by crystal segregation in rapidly cooling melts. *Geochimica et Cosmochimica Acta*, 66**,** 2445–2473.

Publishers: Wrocław University of Technology, Faculty of Geoengineering, Mining and Geology
Polish Meteorite Society

Meteorites
Vol. 1, No. 1, 2011, 29–38
www.meteorites.pwr.wroc.pl
DOI 10.5277/met110104

INVESTIGATIONS OF HAH 286 EUCRITE BY ANALYTICAL ELECTRON MICROSCOPY

Marian SZURGOT[1], Krzysztof POLAŃSKI[2]

[1] Technical University of Łódź, Center of Mathematics and Physics, Al. Politechniki 11, 90 924 Łódź, Poland.
[2] University of Łódź, Department of Solid State Physics, ul. Pomorska 149/153, 90-236 Łódź, Poland.

Abstract: The elemental composition, mineral composition and microstructure of the HaH 286 eucrite found in Lybia in 2000 were studied by analytical electron microscopy. It was established that the mean elemental composition of HaH 286 and atomic and molar ratios: Fe/Mn = 34, Mg/Mg+Fe = 36, Na/Al = 0.066, and Ca/Al = 0.73 are typical of eucrites, and two main meteorite minerals have the mean composition: clinopyroxene En34Fs59Wo7 and plagioclase feldspar An88Ab12. Variations in the composition of pyroxenes and plagioclases are as follows: pyroxene En34-36Fs53-62Wo3-13 and plagioclase: An86-100Ab14-0. Pyroxene is represented by pigeonite and by orthopyroxene. Chromite, ilmenite and silica are minor minerals. The composition, atomic ratios and microstructure indicate that the HaH 286 meteorite is a pyroxene-plagioclase basaltic achondrite, a non-cumulate eucrite with the composition of plagioclase changing between anorthite and bytownite.
Keywords: Eucrite, Hammadah al Hamra 286, analytical electron microscopy, meteorite

INTRODUCTION

Hammadah al Hamra 286 (HaH 286) is one of the Saharan meteorites found in Lybia in 2000. The meteorite was classified as an eucrite in 2001 (Grossman & Zipfel, 2001). Preliminary compositional data for this meteorite are as follows: clinopyroxene Fs28-38Wo32-43, plagioclase An77-92, ferrosilite content 55-60 mol% and shock stage S4 (Grossman & Zipfel, 2001). Studies of thermophysical properties have been recently conducted (Szurgot, 2003, 2011a,b; Szurgot & Wojtatowicz, 2011). Preliminary results of the characterisation of minerals of this HaH meteorite by micro-Raman spectroscopy have been recently published (Szurgot et al., 2011). The aim of this paper is to determine and analyse the elemental and mineral composition of the meteorite and to characterize its microstructure using analytical electron microscopy.

EXPERIMENTAL

The meteorite sample (3g, 32 × 21 × 2.2 mm) was prepared as a polished plate (Fig. 1). The sample was bought from Andrzej Pilski, a well known collector of meteorites. A Tescan VEGA 5135 scanning electron microscope (SEM) and an Axiotech Zeiss optical microscope were used to identify various minerals and to analyze the microstructure and texture of the rock.

The elemental composition of the meteorite was determined by energy dispersive X-ray (EDX) method using an EDX Link 3000 ISIS X-ray microanalyser (Oxford Instruments) with a Si(Li) detector. Oxfords Instruments standards were used for calibration, and a ZAF program was employed for correcting the elemental compositions of minerals. The EDX measurements are accurate to approximately 0.5%.

Elemental X-ray maps of Fe, Al, Ca, Mg, Cr, Si and O were used to create mineral maps and to estimate the modal abundance of the major mineral phas-

Corresponding author: Marian SZURGOT, mszurgot@p.lodz.pl

Fig. 1. Macroscopic view of the HaH 286 meteorite sample. White minerals are plagioclases, gray minerals are pyroxenes.

es – pyroxene and plagioclase, as well as the minor minerals – silica, ilmenite and chromite. The measurement of the relative area occupied by a given mineral, which represents the relative volume of the mineral in the rock, is accurate to roughly 5%.

Back scattered electron (BSE) and optical images of various parts of the meteorite were collected and analyzed. BSE electrons coming from the collimated beam of electrons scattered by the minerals of the sample were collected by YAG scintillator detector. Because the number of counts is directly proportional to the atomic number of the object, the white spots on the image mark the heavy elements, gray spots represent medium elements, and black spots reveal the light elements in the sample (Reed, 2000; Polański, 2008).

RESULTS AND DISCUSSION

Elemental Composition

Figure 2 shows the energy dispersive X-ray spectrum (EDS, EDX spectrum) of the HaH 286 sample and Tab. 1 presents the mean elemental composition of the meteorite. The element content is expressed by weight and atomic percent. A relatively large region of the meteorite (with an area of about 25 mm^2) was irradiated with electrons to generate these X-ray quanta.

Tab. 1 shows that the main chemical components of the meteorite are: Si (21.21 wt%), O (45.18 wt%), Fe (12.80 wt%) and Mg (3.18 wt%), Ca (8.61 wt%), Al (7.89 wt%). They create about 99% of the mass of the minerals constituting the meteorite. Five elements make up remained one percent of the meteorite mass: Na (0.44 wt %), Mn (0.38 wt%), Ti (0.30 wt%), Cr (0.13 wt%) and S (0.1 wt%). Data of Johum and coworkers (Johum et al., 1980) on the elemental composition of the Yamato 74450, Pasamonte and Stannern eucrites are also included in the table. According to the figures, the agreement between our results and

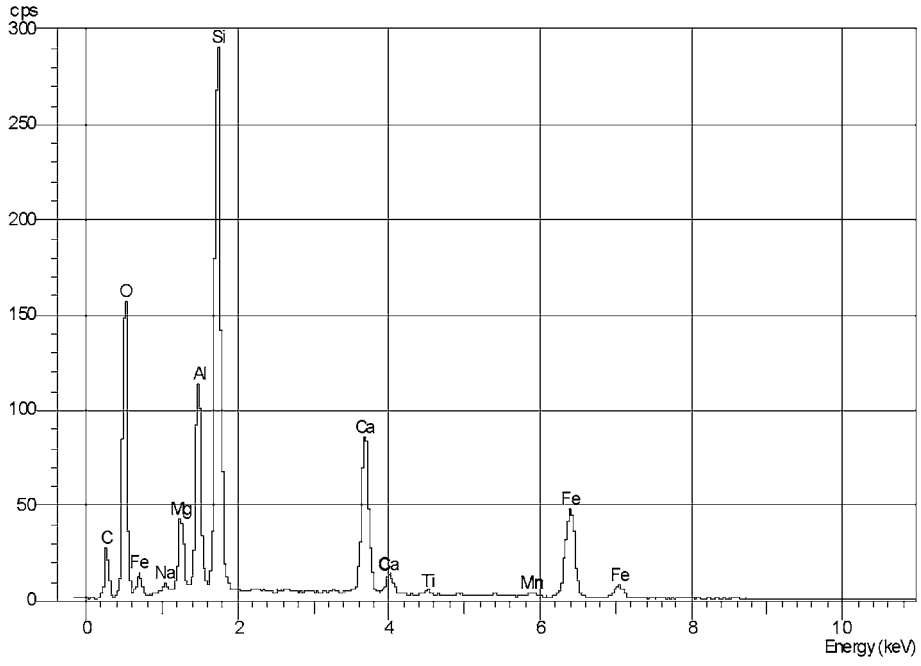

Fig. 2. EDS spectrum of HaH 286 meteorite revealing major elements contributing to the mean bulk composition of the meteorite

Table 1. Mean elemental composition of HaH 286, Yamato 74450, Pasamonte and Stannern eucrites

Element	HaH 286 wt%, (atomic%) (authors own data)	Yamato 74450 wt% (Jochum et al., 1980)	Pasamonte wt% (Jochum et al., 1980)	Stannern wt% (Jochum et al., 1980)
O	45.18 (63.05)	45.5*	44.5*	46.3*
Si	21.21 (16.86)	22.2	23.7	22.5
Mg	3.18 (2.92)	4.2	3.9	4.4
Fe	12.18 (5.12)	13.9	13.4	12.7
S	0.10# (0.07)#	0.13	0.039	0.42
Al	7.89 (6.53)	6.3	6.5	6.0
Ca	8.61 (4.80)	7.0	7.4	7.2
Ni	nd	< 0.04	< 0.04	< 0.04
Na	0.44 (0.43)	0.27	0.31	0.31
Cr	0.13# (0.05)#	0.31	0.14	0.16
Mn	0.38 (0.15)	0.44	0.37	0.33
K	nd	0.041	0.034	0.037
Ti	0.30 (0.14)	ns	ns	ns
Total	100 (100)	100	100	100

*Added to 100 %.

S and Cr content was added since these elements were revealed in another EDS spectrum; nd = not detected, ns = not specified.

literature data for elements present in the HaH 286 meteorite and in eucrites (Jochum et al., 1980; Mittlefehldt et al., 1998; Hutchison, 2004) is satisfactory.

The same conclusion can be drawn from the analysis of atomic ratios for selected elements traditionally used in analyses of eucrites. The Fe/Mn, Ca/Al, Na/Al, mg# = 100 Mg/[Mg+Fe], fe# = 100 Fe/[Mg+Fe], and mg = 100 Mg/[Mg+Fe+Ca] ratios for the HaH 286 meteorite and Y 74450, Pasamonte, and Stannern eucrites are compiled in Tab. 2.

According to the data, Fe/Mn, Ca/Al, Na/Al, mg#, mg, and fe# ratios lie within or close to the range of values established for eucrites (Hutchison, 2004; Mayne et al., 2009; McSween & Huss, 2010, McSween et al., 2011).

Tab. 3 presents the composition of HaH 286 and selected eucrites given by oxide contents (wt %). HaH 286 contains: SiO_2 (46.38%), MgO (5.36%), FeO (16.82%), Al_2O_3 (15.19%), CaO (12.32%), Cr_2O_3 (0.29%), Na_2O (0.51%), MnO (0.49%) and TiO_2 (0.52%). The data show that the mean oxides composition of HaH 286 is within the values exhibited by eucrites (Mason et al., 1979; Johum et al., 1980; Mittlefehldt et al., 1998; Barrat et al., 2000; Hutchison, 2004; Yamaguchi et al., 2009). The MgO content of HaH 286 is somewhat lower, and Al_2O_3 and CaO contents are somewhat higher than in eucrites. S content (0.10 wt%) is of the same order magnitude as in eucrites (0–0.15 wt%), and K_2O and P_2O_5 have not been detected.

The seventh and eighth columns in Tab. 3 indicate that HaH 286 belongs to the basaltic, non-cumulate eucrites (compare TiO_2, Na_2O, and Cr_2O_3 content in HaH 286 with contents of non-cumulate eucrites). The location of the experimental point for HaH 286, TiO_2 content vs. FeO/MgO ratio, in a diagram published by Barrat and coworkers (Barrat et al., 2000), also proves that HaH 286 is a non-cumulate rather than cumulate eucrite. Fig. 3 shows that the location

Table 2. Atomic ratios in HaH 286 and other eucrites

Ratio	HaH 286	Eucrites (Hutchison, 2004)	Yamato 74450 (Jochum et al., 1980)	Pasamonte (Jochum et al., 1980)	Stannern (Jochum et al., 1980)
Fe/Mn	34	30-33	31[1)]	36[1)]	38[1)]
mg#	36	ns	41	40	44
fe#	64	ns	59	60	56
mg	23	ns	29	27	31
Ca/Al	0.73	0.72-0.79	0.75	0.77	0.81
Na/Al	0.066	ns	0.050	0.056	0.061

mg# = 100 Mg/[Mg+Fe]; fe# = 100 Fe/[Mg+Fe]; mg = 100 Mg/[Mg+Fe+Ca].

[1)] Data for Yamato 74450, Pasamonte and Stannern were calculated on the basis of the weight content of elements; ns = not specified.

Table 3. Mean composition (oxides, wt %) of the HaH 286 meteorite and compositions of selected eucrites

Oxide	HaH 286	Sioux County	Stannern	Nuevo Laredo	Serra de Mage	3 cumulate eucrites##	14 noncumulate eucrites*
SiO_2	46.38	49.2#	49.7#	49.5#	48.5#	ns	ns
MgO	5.36	6.88	6.97	5.55	10.7	6.01–8.54##	6.16–7.77*
FeO	16.82	18.4	17,8	19.6	14.4	15.57–19.76	18.28–21.62
S	0.10	0.07	nd	nd	0.15	nd	nd
Al_2O_3	15.19	13.1	12.3	12.2	14.8	6.86–14.77	11.19–14.41
CaO	12.32	10.4	10.7	10.3	9.75	5.87–9.80	9.99–11.12
Na_2O	0.51	0.41	0.62	0.51	0.25	0.25–0.45	0.21–0.59
Cr_2O_3	0.29	0.32	0.34	0.28	0.63	0.41–0.82	0.24–0.38
MnO	0.49	0.55	0.53	0.58	0.48	0.45–0.63	0.48–0.60
K_2O	nd	0.03	0.07	0.05	0.01	nd	nd
P_2O_5	nd	nd	0.10	nd	0.03	nd	nd
TiO_2	0.52	0.58	0.98	0.83	0.13	0.17–0.43	0.54–1.07

Hutchison's data: Sioux County, Stannern, Nuevo Laredo, Serra de Mage (Hutchison, 2004).
##, * Barrat et al., data for 17 eucrites (Barrat et al., 2000).
Cumulates (3 eucrites), * noncumulates (14 eucrites). nd = not detected. ns = not specified.

of HaH 286 (0.52%, 3.1) indicates that the HaH 286 eucrite can be included into the trend line for MG-Nuevo Laredo group of eucrites. TiO_2 content in HaH 286 overlaps with both the main group (MG, with a range of 0.6–0.8 wt%) and the Nuevo Laredo groups of eucrites. Since the MG eucrites have a somewhat lower range of FeO*/MgO ratios, between 2.4 and 2.5 (Barrat et al., 2000), it is likely that HaH 286 is a member of the Nuevo Laredo group of eucrites.

Mineral Composition and Microstructure

Since the elements: Fe, Mg, Si, O, Ca, Al and Na make up over 99 percent of the meteorite by weight (Tab. 1), it is evident that the most common minerals in the meteorite are: calcium-poor pyroxene $(Mg,Fe,Ca)_2Si_2O_6$, and plagioclase feldspar (solid solution of albite $NaAlSi_3O_8$ and anorthite $CaAl_2Si_2O_8$) with a high anorthite content. Orthopyroxene $(Mg,Fe)_2Si_2O_6$ is possible. Ilmenite ($FeTiO_3$) as well as chromite ($FeCr_2O_4$) should also be present as accessory minerals.

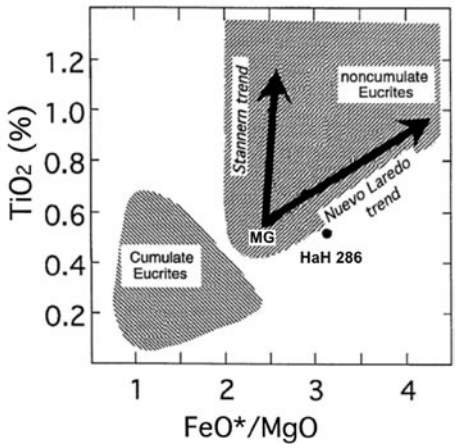

Fig. 3. TiO_2 content versus FeO*/MgO ratio for cumulate and noncumulate eucrites (Barrat et al., 2000). Data for HaH 286 (0.52 wt% of TiO_2, FeO*/MgO = 3.1) reveal that it is a noncumulate eucrite belonging to MG-Nuevo Laredo trend.
FeO* = total FeO.

Si, Mg, Fe, Ca, Al, Na and O contents prove that pyroxene and plagioclase are the dominant minerals in HaH 286. Preliminary identification of clinopyroxenes and plagioclase feldspars in the HaH 286 meteorite was done by Raman spectroscopy (Szurgot et al., 2011). Micro-Raman spectroscopy also revealed the presence of quartz crystals.

Fig. 1 shows an optical image of HaH 286 that reveals the major characteristics of the achondrite: the presence and domination of pyroxene and plagioclase crystals. X-ray maps depicting the distribution of elements and minerals and electron microscope images of HaH 286 are shown in figures 4–8.

Elemental X-ray maps of Fe, Al, Ca, Mg, Si, Cr and O together with the BSE image of the same area of meteorite are presented in Fig. 4. They show that oxygen is distributed more or less uniformly. Iron and magnesium reveal the location of pyroxene crystals and show that pyroxene is a dominant mineral. Plagioclase, is the other major mineral, as seen in the X-ray Al map. The three minerals: chromite located by chromium, silica located with silicon, and ilmenite located via the presence of black patches in the Si map, are minor minerals of the HaH 286 eucrite. Calcium denotes plagioclase, as well as two types of pyroxenes: one with a lower and the other with a higher wollastonite content.

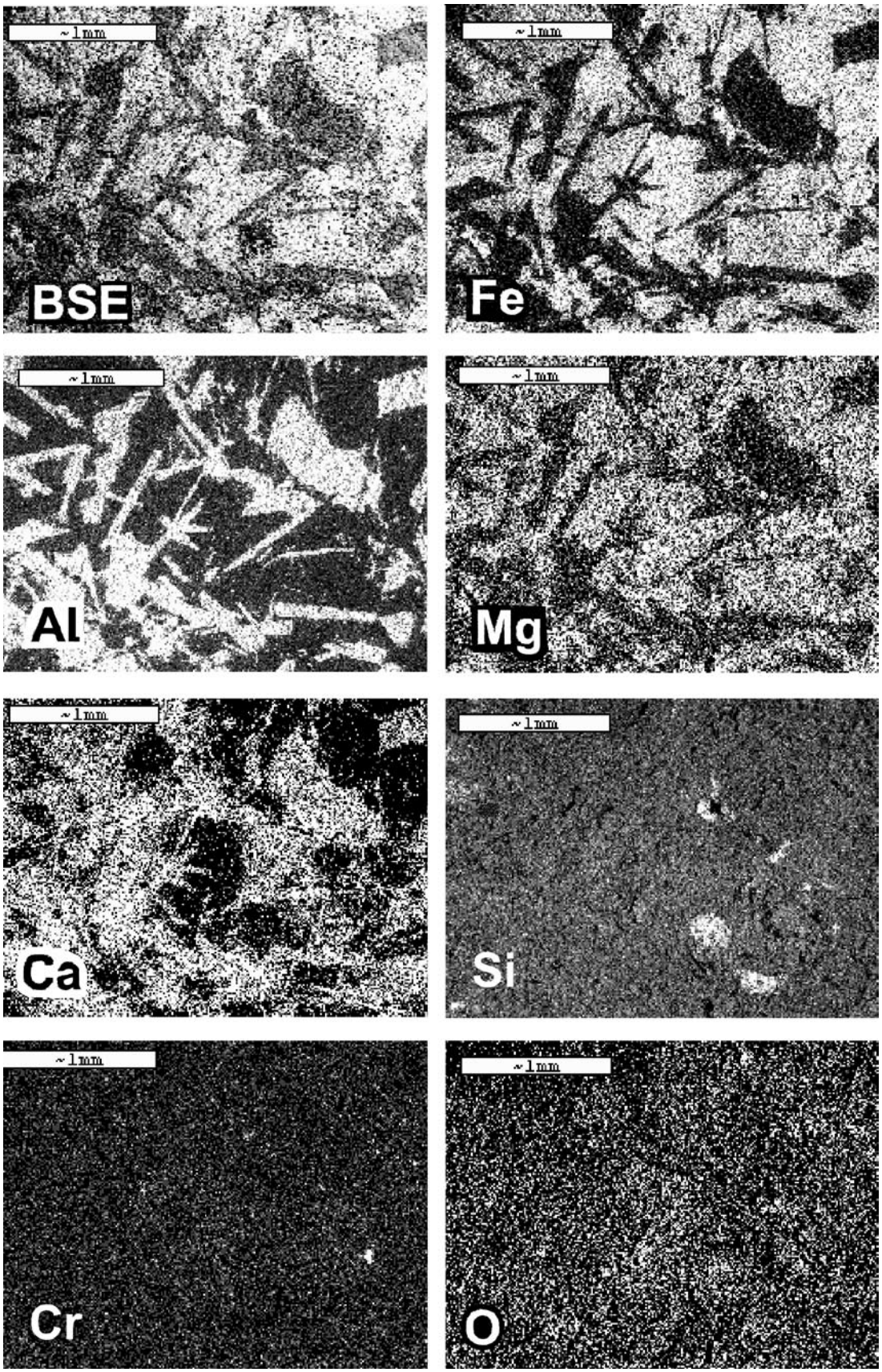

Fig. 4. Backscatter electron image (BSE) and chemical distribution maps (Fe, Al, Mg, Ca, Si, Cr and O) of the HaH 286 meteorite. Oxygen reveals silicates, oxides, and feldspars. Iron and magnesium reveal the location of pyroxene, and aluminium denotes the location of plagioclase crystals. Chromium indicates the location of chromite, and silicon shows the location of silica. Calcium is present in plagioclase and in pyroxenes (some pyroxenes have higher, and some have lower Ca contents). In each X-ray map, the higher density of white spots denotes higher abundances of given elements. Black areas mean that the element is absent

a) b)

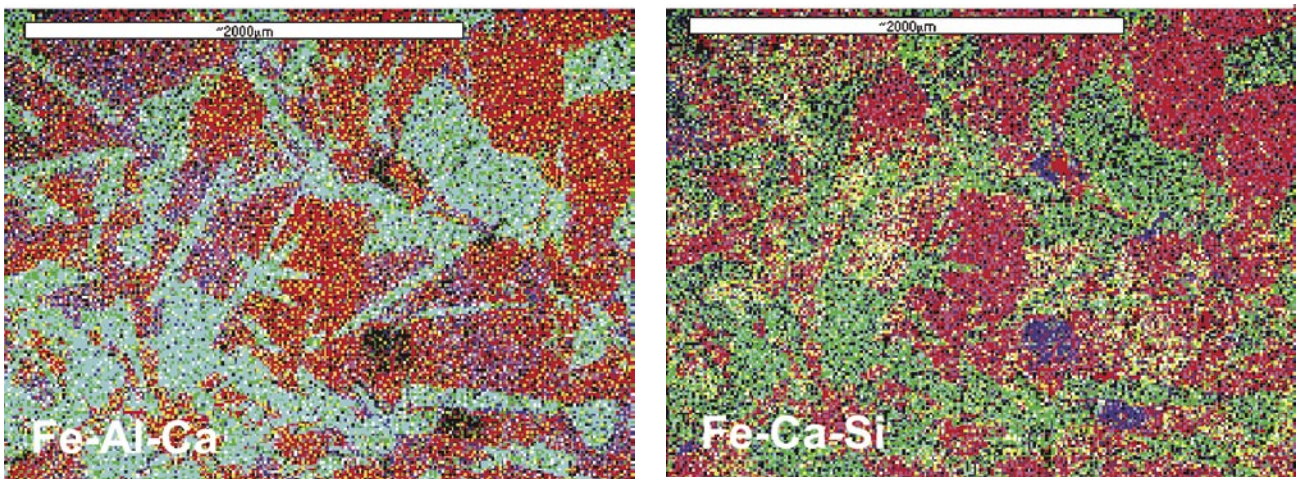

Fig. 5. Mineral maps of the same area of HaH 286 revealing major minerals. Images 5a and 5b consist of superimposed: a) Fe, Al and Ca, and b) Fe, Ca and Si elemental X-ray maps. Colour of elements: a) Fe is red, Al is green and Ca is blue, b) Fe is red, Ca is green, and Si is blue. Colour of minerals: a) pyroxene with lower Ca content is red, and pyroxene with higher Ca content is lilac, plagioclase is blue-green (cyan), and silica is black, b) pyroxene with lower Ca content is purple, and pyroxene with higher Ca content is yellow, plagioclase is green, and silica is blue

Fig. 5 shows two mineral maps of the same area of HaH 286. The images were created by superimposing X-ray maps of representative elements. The two mineral maps presented in Figs. 5a and 5b consist of superimposed: a) Fe, Al, and Ca and b) Fe, Ca and Si elemental X-ray maps. In Fig. 5a, pyroxene with lower Ca contents is red, pyroxene with higher Ca contents is lilac, plagioclase is cyan-green, and silica is black. In Fig. 5b pyroxene with lower Ca contents is purple, and pyroxene with higher Ca contents is yellow, plagioclase is green and silica is blue.

The X-ray elemental and mineral maps enabled us to estimate the modal composition of HaH 286 eucrite. According to our data, HaH 286 contains: pyroxene (54 vol%), plagioclase (44 vol%), silica (1 vol%), ilmenite (0.8 vol%), and chromite (0.1 vol%) (Tab. 4). Troilite content estimated by optical microscopy is about 0.1%. Tab. 4 shows that the modal composition of HaH 286 classifies this meteorite as a basaltic, nonocumulate eucrite (compare the mineral content of HaH 286 with the contents commonly seen in basaltic eucrites).

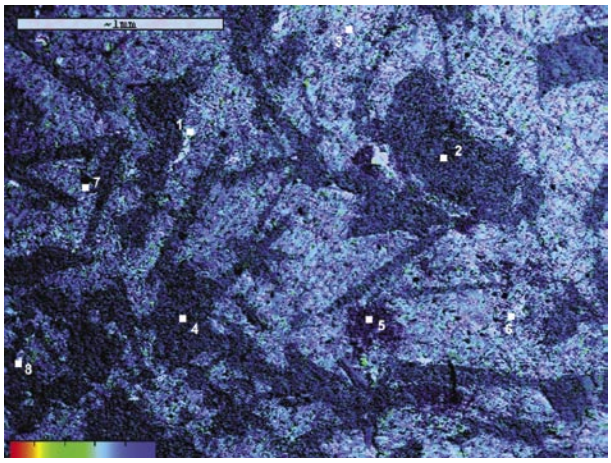

Fig. 6. X-ray Cameo image of the same region of HaH 286 as that shown in Figs 4 and 5. 1 – ilmenite, 2 – An87, 3 – En36Fs58Wo6, 4 – An94, 5 – silica, 6 – En34Fs53Wo13, 7 – En91Fs7Wo1, 8 – An90. The colour scale red-green-blue represents X-ray energy in the range between 0.2 keV (red) and 5 keV (blue). Blue represents Ca content: dark-blue means higher Ca content, and light-blue, lower Ca content. Green represents S and Si. Field of view: 3 × 2.2 mm

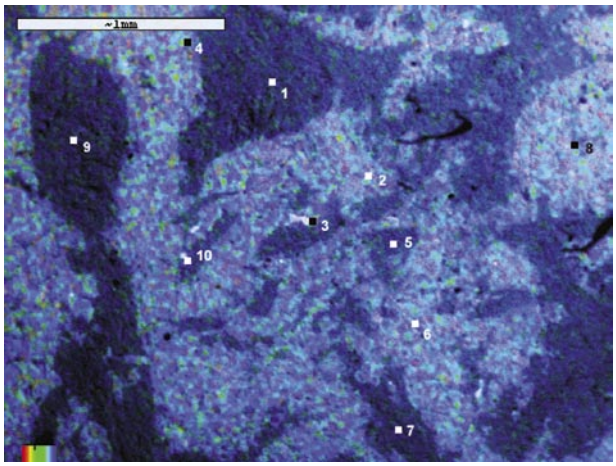

Fig. 7. X-ray Cameo image of another region of HaH 286. 1 – An90, 2 – En37Fs57Wo6, 3 – chromite and ilmenite, 4 – En35Fs62Wo3, 5 – An88, 6 – En35Fs55Wo10, 7 – An86, 8 – En34Fs62Wo4, 9 – An100, 10 – chromite and ilmenite. The colour scale red-green-blue represents X-ray energy in the range between 0.6 keV (red) and 1.75 keV (blue). In this scale, blue represents Si content, green, Mg content, and red represents Fe, Ti, and Cr content. Field of view: 3 × 2.2 mm

Table 4. Modal composition of HaH 286 and basaltic eucrites

Mineral	HaH 286	22 Eucrites (Delaney et al., 1984)	26 Eucrites (Mayne et al., 2009)	Eucrites (Hutchison, 2004)
Pyroxene	54	51.3 ± 2.6* [47.5–56.2]	49.9 ± 5.4* [38–60]	[63–50]
Plagioclase	44	43.1 ± 2.1 [39.4–46.6]	45.7 ± 6.1 [35–61]	[30–47]
Silica	1	4.0 ± 1.5 [1.1–7.7]	3.2 ± 2.7 [0–12]	[1–4.7]
Ilmenite	0.8	0.8 ± 0.3 [0.3–1.5]	ns	[tr–3.3]
Chromite	0.1	0.2 ± 0.2 [tr–0.5]	ns	[tr–0.6]
Troilite	0.1##	0.4 ± 0.3 [tr–1.1]	ns	[tr–0.5]
Fe Metal	nd	tr [tr–0.3]	ns	[tr–0.5]
Phosphate	nd	0.2 ± 0.1 [tr–0.4]	ns	[tr–0.3]
Fayalite	nd	ns	ns	[0–tr]
OSM**	1#	1.4±0.8#	0. 9 ± 0.7 [0–3]	ns

* Average of 22 eucrites (Delaney et al., 1984) and of 26 eucrites (Mayne et al., 2009) together with the standard deviation.
**OSM = oxide + sulfide + metal.
The sum of ilmenite, chromite, troilite and Fe metal, specified in upper rows as separate phases.
[ ] The range of values; nd = not detected; ns = not specified; tr = trace (< 0.1 vol%).
The modal abundance of troilite was estimated by optical microscopy. Pyroxene = orthopyroxene, pigeonite and augite.

The energy dispersive (EDS) spectra revealed (apart from the mean) the local composition of the meteorite. Pigeonite, with the compositions En36Fs58Wo6, En37Fs57Wo6, En35Fs55Wo10, En34Fs53Wo13, is commonly present in the meteorite (Figs. 6, 7). Data presented in Tab. 1 enabled us to determine the mean composition of pigeonite in the meteorite. Pigeonite's mean composition is En34Fs59Wo7, and the range of local compositions is En34–36Fs53–62Wo3–13. Data presented in Tab. 5 show that pigeonite is Fe-rich, and that its composition is characteristic of basaltic eucrites. This is seen in a pyroxene quadrilateral diagram. However, Figs 5, 6, 7 and Tab. 5 show that, apart from clinopyroxene pigeonite, orthopyroxene (En35Fs62Wo3, En34Fs62Wo4, and even En91Fs7Wo1) also occurs in the HaH 286 meteorite. The X-ray maps shown in Figs. 4 and 5 revealed two pyroxenes, one with higher wollastonite (Wo) content, and one with lower Wo content. These results suggest that the grains are clinopyroxene pigeonite (Px with higher Wo content), and orthopyroxene (Px with lower Wo content).

EDS spectra enabled us to identify and determine the composition of plagioclase in the HaH 286 meteorite. According to data presented in Tab. 1, the mean composition of the plagioclase in the meteorite is An88Ab12. Local analyses revealed that anorthite contents of plagioclase span a wide range of values from An86 to An100 (An86–100Ab14–0). Figs 6 and 7, in addition to Tab. 5, show that HaH 286's plagioclase composition is as follows: An86Ab14, An87Ab13, An88Ab12, An90Ab10, and An100Ab0. Apart from the two dominant minerals, pyroxene and plagioclase, minor minerals typical of eucrites have been revealed in HaH 286: silica, ilmenite and chromite. HaH 286 can be classified as a basaltic eucrite.

BSE images also reveal the aforementioned minerals present in this meteorite sample. White patches and veins in Fig. 8 are ilmenite and chromite, light grey areas in this BSE image are pyroxene, darker areas are plagioclase, and nearly black areas are silica, as expected for this type of meteorite. This mineral composition is consistent with the mineral composition resulted from interpretation of the X-ray maps

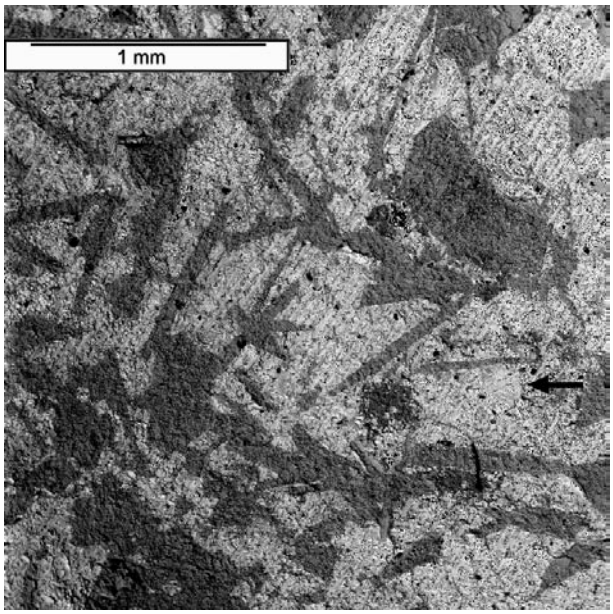

Fig. 8. BSE image of the HaH 286 eucrite revealing the constituent minerals and texture of the meteorite. Pyroxene crystals in this image are light grey and medium grey, plagioclase is dark grey, silica is black, and ilmenite and chromite are white. Arrow indicates a pigeonite crystal exhibiting compositional zoning

Table 5. Composition of plagioclases and pyroxenes in HaH 286

Mineral	HaH 286	Basaltic Eucrites (Mayne et al., 2009; McSween et al. ,2011)
Plagioclase	An88Ab12 (mean)	
	An86Ab14 An87Ab13 An88Ab12	
	An90Ab10	
	An90Ab10	
	An100	
	An86–100 (range)	An73–96
Pyroxene	En34Fs59Wo7 (mean)	
Clinopyroxene	En36Fs58Wo6	
	En37Fs57Wo6	
	En35Fs55Wo10	
	En34Fs53Wo13	
	En34–37Fs53–58Wo6–13 (range)	
Orthopyroxene	En91Fs7Wo1	
	En35Fs62Wo3	
	En34Fs62Wo4	
	En34–91Fs7–62Wo1–3 (range)	

(Figs. 4–7). HaH 286 displays a subophitic to ophitic texture consisting of lath-shaped plagioclase and anhedral, irregular pyroxene. Certain plagioclase crystals occur as radiating sprays of lath-shaped grains enclosed by larger pyroxene grains. Ilmenite occurs either as a separate phase or is associated with chromite (points 3 and 10 in Fig. 7). The coexistence of ilmenite and chromite may indicate that ilmenite was reduced to chromite. Certain pyroxenes display zonation with an exsolved texture with coarsely spaced lamellae (Fig. 8). In general, the texture of HaH 286 is typical of pyroxene-plagioclase achondrites known as eucrites (Stolper, 1977; Yamaguchi et al., 1997; Takeda, 1997; Takeda et al., 1997; Mittlefehldt et al., 1998; McSween, 1999; Norton, 2002; Hutchison, 2004; Mayne et al., 2009; McSween et al., 2011).

Fig. 8 shows laths of plagioclase crossing pigeonite and orthopyroxene crystals. The plagioclase must have grown while much of the magma was still liquid (Wasson, 1985). This structure demonstrates the origin of HaH 286 due to crystallization from a melt. This means that HaH 286 represents an igneous type rock, i.e. the rock crystallized from the magma formed by melting in the processes called partial melting, in which terrestrial and extraterrestrial basalts were created. The plagioclase crystallized from the melted material of similar composition, and their lathlike shape is the result of slow cooling (Wasson, 1985). The pyroxenes must have started to crystallize at about the same time as the plagioclase, and their equidimensional crystals ended up between the long plagioclase crystals (Wasson, 1985). HaH 286's texture can be classified as ophitic or subophitic since it resembles the texture of igneous rocks in which randomly oriented plagioclase crystals are surrounded by large pyroxene crystals. But, HaH 286 also exhibits equidimensional, coarse, anhedral plagioclase crystals coexisting with anhedral, irregular pyroxene crystals (Fig. 7). Remelting of the rock during shock collision(s) may have caused this texture. According to Grossman and Zipfel, HaH 286 is a moderately shocked meteorite, with a shock stage of S4 (Grossman & Zipfel, 2001). This indicates that HaH 286 has undergone metamorphic recrystallization, as have most HED achondrites. Impact metamorphism (breccia formation and rapid heating followed by slow cooling) led to the modification of these meteorites' original textures and mineral composition, but even highly metamorphosed eucrites have retained their initial bulk compositions (Mittlefehldt & Longhi, 1998).

An analysis of the molar ratios Fe/Mn and Fe/Mg in HaH 286 provides evidence that the meteorite belongs to the evolved achondrites rather than to the primitive achondrites. This conclusion is based on Goodrich and Delaney's results, in which they noted that primitive achondrites, exhibiting metamorphic textures appropriate for solid residues from which melts were extracted, can be readily distinguished from magmatic achondrites (SNCs, HEDs, and lunar basalts) using a diagram of molar Fe/Mn versus Fe/Mg (Goodrich & Delaney, 2000; McSween & Huss, 2010). The diagram is shown in Fig. 9. Primi-

tive achondrites have Mn/Mg ratios distinctly different from evolved, magmatic achondrites, and the Mn/Mg ratio of magma can change during the process of fractional crystallization (Goodrich & Delaney, 2000; McSween & Huss, 2010). The evolved achondrites exhibit a nearly constant Fe/Mn ratio. In Fig. 9, the PA trend line represents data for primitive achondrites (lodranites, acapulcoites, winonaites, brachinites, and ureilites), and the MA trend line (with the small slope) represents data for evolved, magmatic achondrites (HEDs and SNCs). The field of magmatic achondrites is marked as the area between the two dashed lines. Figure 9 shows that the experimental point (Fe/Mn = 34, Fe/Mg = 1.75) representing HaH 286 meteorite is located within the field of magmatic HED achondrites (the lunar basalt field located above the HED field is not drawn here).

The Fe/Mn ratio in pyroxenes is diagnostic for determining a common planetary origin of meteorites, as the primordial values of these elements are believed to remain constant through planetary differentiation (Papike, 1998; Papike et al., 2003; Mayne et al., 2009). Recent data on Fe/Mn – Fe/Mg relations for twenty-nine unbrecciated eucrites show that it is possible to distinguish between cumulate and noncumulate eucrites (Mayne et al., 2009). Our data for HaH 286 indicate that this achondrite belongs to the noncumulate eucrites since HaH 286 (shown in Fig. 9) is located within the field of noncumulates.

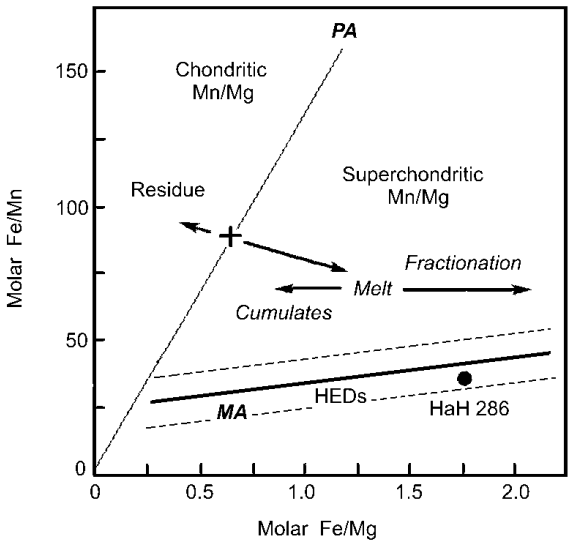

Fig. 9. Diagram used to distinguish between achondrites crystallizing from melts (evolved achondrites) and primitive achondrites, representing the solid residue from extracted melt (Goodrich & Delaney, 2000; McSween & Huss, 2010). Line MA represents the trend for magmatic, evolved achondrites, and line PA represents the trend for primitive achondrites. Notice that the experimental point (filled circle) for the HaH 286 achondrite (Fe/Mn = 34, Fe/Mg = 1.75) is located within the field of magmatic achondrites

Table 6. Thermophysical properties of HaH 286

Property	HaH 286 value
Specific heat capacity (Szurgot, 2003)	657 J kg^{-1} K^{-1}
Thermal conductivity (Szurgot, 2011b)	1.9 W m^{-1} K^{-1}
Thermal diffusivity (Szurgot & Wojtatowicz, 2011)	$0.93 \cdot 10^{-6}$ m^2 s^{-1}
Bulk density (Szurgot, 2003)	3.13 g cm^{-3}

Physical properties of HaH 286

In Tab. 6, data on bulk density and thermophysical properties of HaH meteorite have been compiled (Szurgot, 2003, 2011a,b; Szurgot & Wojtatowicz, 2011). They show that the bulk density, specific heat capacity, thermal diffusivity and thermal conductivity of HaH 286 are characteristic of a basalt.

CONCLUSION

All identified minerals are characteristic of eucrites. Elemental, oxide and modal composition data and microstructure, indicate that the HaH 286 meteorite is a pyroxene-plagioclase basaltic achondrite, one of the non-cumulate eucrites.

ACKNOWLEDGEMENTS

We would like to express our gratitude to Professor Tadeusz Przylibski for the valuable comments on the manuscript and encouragement, and also to the anonymous reviewers for their valuable suggestions and comments.

REFERENCES

Barrat J.A., Blichert-Toft J., Gillet PH., Keller F., 2000 – The differentiation of eucrites: the role of in-situ crystallization, *Meteoritics & Planetary Science*, 35, 1087–1100.

Delaney J.S., Prinz M., Takeda H., 1984 – The polymict eucrites. *Journal of Geophysical Research*, 89, *Supplement,* C251––C288.

Goodrich C.A., Delaney J.S., 2000 – Fe/Mg-Fe/Mn relations of meteorites and primary heterogeneity of primitive achondrite parent bodies. *Geochimica et Cosmochimica Acta*, 64, 149–160.

Grossman J.N., Zipfel J., 2001 - Meteoritical Bulletin, no 85, 2001 September. *Meteoritics & Planetary Science*, 36, A293––A322.

Hutchison R., 2004 – Meteorites: A petrologic, chemical and isotopic synthesis. Cambridge University Press, Cambridge, UK.

Johum K.P., Grais K.I., Hintenberger H., 1980 – Chemical composition and classification of 19 Yamato meteorites. *Meteoritics*, 15, 31–39.

Mason B., Jarosevich E., Nelen J.A., 1979 – The pyroxene-plagioclase achondrites. *Smithsonian Contributions to the Earth Sciences*, 22, 27–45.

Mayne R.G., McSween H.Y., McCoy T.J., Gale A., 2009 – Petrology of the unbrecciated eucrites. *Geochimica et Cosmochimica Acta*, 73, 794–819.

McSween H.Y., Jr., 1999 – Meteorites and their parent planets. Cambridge University Press, Cambridge, UK.

McSween H.Y., Jr., Huss G.R., 2010 – Cosmochemistry. Cambridge University Press, Cambridge, UK.

McSween Jr. H.Y., Mittlefehldt D.W., Beck A.W., Mayne R.G., McCoy T.J., 2011 – HED meteorites and their relationship to the geology of Vesta and the Dawn mission. *Space Science Reviews*, 163, 141–174.

Mittlefehldt D.W., Longhi J. 1997 – Basaltic achondrite meteorites, [in:] Shirley J.H., Fairbridge H. (eds), *Encyclopedia of Planetary Sciences*, Chapman & Hall, London, 65–68.

Mittlefehldt D.W., McCoy T.J., Goodrich C.A, Kracher A., 1998 – Non-chondritic meteorites from asteroidal bodies, [in:] Papike J.J. (ed.), *Planetary materials,* Mineralogical Soc. America, Washington, 4.1–4.195.

Norton O.R., 2002 – The Cambridge encyclopedia of meteorites. Cambridge University Press, Cambridge, UK.

Papike J.J, 1998 – Comparative planetary mineralogy: chemistry of melt-derived pyroxene, feldspar, and olivine, [in:] Papike J.J. (ed.), *Planetary materials,* Mineralogical Soc. America, Washington, 7.1–7.11.

Polański K., 2008 – Analytical electron microscopy in crystals investigations, [in:] Wojtczak L. and Ziomek J. (eds), *Crystals in nature and technology,* University of Lodz, Łódź, 173–190 (in Polish).

Reed S.J.B., 2000 – Electron microprobe analysis and scanning electron microscopy in geology, Cambridge University Press, Cambridge, UK.

Stolper E., 1977 – Experimental petrology of eucritic meteorites. *Geochimica et Cosmochimica Acta*, 41, 587–611.

Szurgot M., 2003 – Thermophysical properties of meteorites, Specific heat capacity. *2nd Meteorite Seminar in Olsztyn*, 136–145 (in Polish).

Szurgot M., 2011a – On the specific heat capacity and thermal capacity of meteorites. *42nd Lunar and Planetary Science Conference,* Abstract #1150.pdf

Szurgot M., 2011b – Thermal conductivity of meteorites. *Meteoritics & Planetary Science*, 46, *Supplement*, A230.

Szurgot M., Wojtatowicz, T.W., 2011 – Thermal diffusivity of meteorites. *Meteoritics & Planetary Science*, 46, *Supplement,* A230.

Szurgot M., Tomasik A., Kozanecki M., 2011 – Identification of minerals in HaH 286 eucrite by Raman spectroscopy. *53rd Polish Crystallographic Meeteing in Wrocław,* 278–279 (in Polish).

Takeda H., 1997 – Mineralogical records of early planetary processes on the howardite, eucrite, diogenite parent body with reference to Vesta. *Meteoritics & Planetary Science*, 32, 841–853.

Takeda H., Ishi T., Arai T., Miyamoto M., 1997 – Mineralogy of the Asuka 87 and 88 eucrites and crustal evolution of the HED parent body. *Antarctic Meteorite Research*, 10, 401–413.

Wasson J.T, 1985 – Meteorites, their record of early solar-system history. Freeman and Comp., New York, USA.

Yamaguchi A., Taylor G.J., Keil K., 1997 – Shock and thermal history of equilibrated eucrites from Antarctica. *Antarctic Meteorite Research*, 10, 415–436.

Yamaguchi A., Barrat J.A., Greenwood R.C., Shirai N., Okamoto C., Setoyanagi T., Ebihara M., Franchi I.A., Bohn M., 2009 – Crustial partial melting on Vesta: evidence from highly metamorphosed eucrites. *Geochimica et Cosmochimica Acta*, 73, 7162–7182.

Publishers: Wrocław University of Technology, Faculty of Geoengineering, Mining and Geology
Polish Meteorite Society

GUIDELINES FOR AUTHORS

Meteorites publishes only original works that have not been previously published in any journal, joint publication, conference materials, on the Internet, or in any other citable form, and that are not under consideration by other publications at the time of submission. Authors must own the copyright to the data, tables, figures and appendices. Manuscripts accepted for publication in Meteorites (and excerpts) must not be published in any periodical in any language without the permission of the editor-in-chief.

Authors are asked to communicate their contact details (including their e-mail addresses) to the editorial staff and two potential reviewers. Papers must be written in English. Authors are expected to have the papers reviewed linguistically prior to submitting. Papers should be prepared using Microsoft Word 97 or a later version. Figures must be provided in a jpg format with a printable version of at least 400 dpi. Only electronic submissions through e-mail will be accepted.

Italics should be used for equations and formulas only. Decimals should be separated with a point instead of a comma, and a space should be used as a thousands separator. Double or triple line spacing should be used and ample margins of at least 3 cm should be employed. The text should be justified and words should not be divided at the end of a line.

Tables and figures must be prepared on separate pages and not included as part of the main text. They must be numbered in Arabic numerals according to their sequence in the text. Captions to tables and figures must be placed at the end of the manuscript, after the references.

Appendices will be published by way of exception only and may include, but are not limited to, large tables with numerical or analytical results, or the sources of data used for the analysis. Equations and formulas must be centered and numbered consecutively and their numbers must be written on the right, justified in parentheses. Variables and constants should be defined under equations and formulas. Refer to the example below.

$$v > \sqrt{\frac{2MG}{r}} \qquad (1)$$

where:

v – escape velocity, $m \cdot s^{-1}$,

M – mass of body from which object is projected, kg,

G – universal gravitational constant, $N \cdot m^2 \cdot kg^{-2}$,

r – radius of body from which object is projected, m.

The manuscript title should be bold and capitalized, e.g.: **ACHONDRITES AND THEIR PARENT BODIES**. Full name of the author(s) should be given below the title, followed by their affiliation(s), and exact postal address. In the case of a paper with more than one author, correspondence concerning the paper will be sent to the first author unless the editorial staff is advised otherwise by an underlining of the relevant name(s). First name should be given first and the initials of middle names and the surname, thereafter, e.g.: Tadeusz A. PRZYLIBSKI.

The abstract of up to 300 words and keywords of up to 9 words must be provided. Paper should be divided into sections, described by short headings. Section headings should be capitalized, e.g.: INTRODUCTION, EXPERIMENTAL / METHODS, DISCUSSION, CONCLUSIONS, etc. Acknowledgments may be included after the body of the text before the references.

Mineral and meteorite names used in the paper must conform to the current nomenclature guidelines of the International Mineralogical Association and the Meteoritical Society. If the name of a particular meteorite has not been officially recognized yet, an announcement will have to be published in Meteorites following its approval.

The "0.0" value must not be used for immeasurably small amounts of particles. The "n.d." (not detected or no data) or "n.a." (not available) abbreviations should instead be used.

CITING SOURCES

Cited sources should be enclosed within parentheses. The author's name and the year of publication should be separated by a comma. Papers with more than two authors should be cited by the first author's last name followed by „et al.", and then the year of publication. If the particular author has two or more texts published in the same year, add a letter after the year to distinguish between them. The same letter should be included in the list of works cited at the end of the paper. See the examples below which will be further used in the bibliography section.

(Rubin, 2003)
(Hutchison, 2004)
(Consolmagno & Britt, 2004)
(Przylibski et al., 2005)

PREPARING REFERENCES

References should be arranged alphabetically. Multiple citations of the same author should be listed chronologically. Works by two authors should be cited by using their last names and should be arranged alphabetically by the names of the authors. Multiple papers by the same author having the same publication date should be distinguished by consecutive letters of the alphabet commencing with "a". Multiple publications with the same co-author should be listed chronologically. See the examples below.

Rubin A.E., 2003 – Chromite-Plagioclase assemblages as a new shock indicator; implications for the shock and thermal histories of ordinary chondrites. *Geochimica et Cosmochimica Acta*, 67 (14), 2695–2709.

Hutchison R., 2004 – Meteorites: A petrologic, chemical and isotopic synthesis. Cambridge University Press, New York.

Consolmagno G.J., Britt D.T., 2004 – Meteoritical evidence and constraints on asteroid impacts and disruption. *Planetary and Space Science*, 52 (12), 1119–1128.

Przylibski T.A., Zagożdżon P.P., Kryza R., Pilski A.S., 2005 – The Zakłodzie enstatite meteorite: Mineralogy, petrology, origin, and classification. *Meteoritics & Planetary Science*, 40 (9), Supplement, A185–A200.

Please refer to the latest issue in case of any doubts regarding the preparation of the manuscript.

Proofs will be sent as a PDF file to the e-mail address of the corresponding author. Only minor changes that do not alter the arrangement of the text and corrections of editorial errors will be allowed at this stage. Substantial changes to the text will not be accepted. Proofs should be returned to the editorial staff within seven calendar days. A PDF file of the article will be sent free of charge to the corresponding author immediately after publication.

COPYRIGHT INFORMATION

The author retains the larger portion of the copyright. The following applications of the article are not subject to the editorial staff's opinion or approval:

- making hard and electronic copies of the article for the personal use of the author, including the personal use connected with teaching,
- making copies of the article for the personal use of the author's colleagues from similar fields of research,
- presentation of the article to any forum (conference, symposium or other official meeting) and the document's distribution among its participants,
- obtaining patents based on information contained in the article,
- re-use of all or part of the published article in the author's doctoral thesis or other scientific thesis for a degree,
- re-use of all or part of the published article in compilations of the author's publications,
- re-use of all or part of the published article in books on the condition that a reference is made to the first publication of the article.

Crew

Table of Contents

Krzesińska A., High resolution X-ray tomography as a tool for analysis of internal textures in meteorites 3

Semenenko V.P., Girich A.L., Shkurenko K.O., Kychan N.V., Shyrinbekova S.N., Gorovenko T.M., Nanometer-sized mineral grains and their genetic types in meteorites . . 13

Karwowski Ł., Pilski A.S., Muszyński A., Arnold S., Notkin G., Gurdziel A., New finds in the Morasko meteorite preserve, Poland 21

Szurgot M., Polański K., Investigations of HaH 286 eucrite by analytical electron microscopy 29

www.meteorites.pwr.wroc.pl